

1

2 **Incorporating seed fate into plant-frugivore networks increases**
3 **interaction diversity across plant regeneration stages**

4

5

6 ISABEL DONOSO*, DANIEL GARCÍA, JAVIER RODRÍGUEZ-PÉREZ, AND
7 DANIEL MARTÍNEZ

8 Depto. Biología de Organismos y Sistemas, Universidad de Oviedo, and Unidad Mixta
9 de Investigación en Biodiversidad (UMIB, CSIC-Uo-PA), E-33071 Oviedo, Spain

10 * Corresponding author: idonoso002@gmail.com

11

12

13 **ABSTRACT**

14 Plant-animal mutualistic interactions, such as pollination and seed dispersal, affect
15 ecosystem functioning by driving plant population dynamics. However, little is known
16 of how the diversity of interactions in these mutualistic networks determines plant
17 regeneration dynamics. To fill this gap, interaction networks should not only account
18 for the number of seeds dispersed by animals, but also for seed fate after dispersal.
19 Here, we compare plant-animal networks at both the seed dispersal and seedling
20 recruitment stage to evaluate how interaction diversity, represented by different network
21 metrics, changes throughout the process of plant regeneration. We focused on a system
22 with six species of frugivorous birds and three species of fleshy-fruited trees in the
23 temperate secondary forest of the Cantabrian Range (N Iberian Peninsula). We
24 considered two plant cohorts corresponding to two fruiting years showing strong
25 differences in fruit and frugivore abundance. Seed dispersal interactions were estimated
26 from a spatially-explicit, field-validated model predicting tree and bird species-specific
27 seed deposition in different microhabitats. These interactions were further transformed
28 into interactions at the seedling recruitment stage by accounting for plant- and
29 microhabitat-specific seed fates estimated from field sampling. We found that network
30 interaction diversity varied across plant regeneration stages and cohorts, both in terms
31 of the evenness and the number of paired interactions. Tree-bird interactions were more
32 evenly distributed across species pairs at the recruitment stage than at the seed
33 deposition stage, although some interactions disappeared in the seed-to-seedling
34 transition for one plant cohort. The variations in interaction diversity were explained by
35 between-plant differences in post-dispersal seed fate and in inter-annual fruit
36 production, rather than by differences between frugivores in seed deposition patterns.

- 37 These results highlight the need for integrating plant traits and disperser quality to
- 38 predict the functional outcome of plant-animal mutualistic networks.

39 INTRODUCTION

40 Plant-animal mutualistic networks (e.g. flowering plants and pollinators; fruiting plants
41 and frugivores providing seed dispersal) are assumed to affect ecosystem functioning by
42 controlling vegetation dynamics (Blütghen and Klein 2011, Schleuning et al. 2015).
43 Despite the recent interest in the structure of such networks (e.g. Bascompte and
44 Jordano 2007, Schleuning et al. 2012), we are still far from understanding their
45 functional effects. This is because the quantitative descriptions provided by interaction
46 frequencies (e.g. number of pollen grains or seeds transported by the animals) may tell
47 little about the concomitant demographic expectancies of animals and plants (but see
48 Vázquez et al. 2007, Vázquez et al. 2012). This constraint is especially challenging in
49 plant-frugivore networks, where post-dispersal seed fate filters any quantitative effect of
50 frugivores on plants (Wang and Smith 2002, Schupp et al. 2010). Seed fate may be
51 under the control of animals, and frugivore species may differ in their quality as
52 dispersers because, for example, they differentially modify seed germination due to gut
53 passage, or they drop seeds in microhabitats with different conditions for seed and
54 seedling survival (Schupp et al. 2010, Mello et al. 2014). In fact, these qualitative
55 differences may actually equalize the role of frugivores in interactions networks, for
56 example, when a rare disperser species drops seeds in microhabitats optimal for plant
57 recruitment (Carlo and Yang 2011, Schleuning et al. 2015). Nevertheless, the variability
58 **in plant traits** affecting seed fate may also drive the functional prominence of plants in
59 networks. For example, plants consumed in small quantities by frugivores but with high
60 probabilities of survival after dispersal (e.g. due to their seed size, low susceptibility to
61 predators or shade tolerance; García et al. 2005a, Xiao et al. 2015), will be more
62 represented in networks, irrespective of the disperser. In sum, we could expect changes
63 in the frequencies of each frugivore and plant species from seed dispersal to recruitment

64 stages when accounting for seed fate which, in turn, could be determined by both
65 disperser quality and plant traits. When seen as a whole, for example by means of
66 interaction-diversity network metrics (e.g. Plein et al 2013; Chama et al. 2013), these
67 global changes in interaction frequencies may be highly informative regarding the final
68 distribution of the effects of frugivores on plant communities. Nevertheless, the
69 prevalence and the mechanisms of changes in interaction diversity across plant
70 regeneration stages remain empirically undemonstrated (but see Schleuning et al. 2015;
71 for a conceptual model).

72 Here, we focus on the plant-frugivore system composed of three fleshy-fruited
73 tree species and six avian seed dispersers in the temperate forest of the Cantabrian
74 Range (N Iberian Peninsula). This assemblage is suitable for evaluating changes in
75 seed-dispersal networks because the plants differ in their post-dispersal seed fate (e.g.
76 susceptibility to seed predators, García et al. 2005a), and dispersers are expected to
77 differ in quality proved that they differed in spatial behaviors (García et al. 2013,
78 Morales et al. 2013). Our general objective was to assess the global patterns of plant
79 recruitment by evaluating the structure of plant-frugivore networks after incorporating
80 plant demography (i.e. seed and seedling fate). We first estimated the seed deposition of
81 fleshy-fruited trees by bird species, in different microhabitats, as predicted by a
82 spatially-explicit, field-validated mechanistic model. We assumed that the quality of
83 seed dispersers was mostly determined by the deposition microhabitat. Then, we
84 transformed seed deposition into seedling recruitment by accounting for species and
85 microhabitat-specific seed fate, estimated from field sampling. Specifically, we
86 compared the structure of networks across the seed dispersal and the seedling
87 recruitment stages, by means of metrics representing interaction diversity. Given that
88 the study system can show strong inter-annual differences in the abundance of both

89 birds and fruits (García et al. 2013), we also compare the networks from two years,
90 representing two different plant demographic cohorts, as well as two landscape
91 scenarios of fruit availability.

92

93 MATERIAL AND METHODS

94 *Study system*

95 This study is focused on a plant-frugivore system composed of fleshy-fruited trees and
96 birds in the temperate secondary forest of the Cantabrian Range (northern Iberian
97 Peninsula). This is a common habitat showing low cover and a high degree of
98 fragmentation due to anthropic pressure (García et al. 2005b). It is dominated by
99 hawthorn (*Crataegus monogyna*), holly (*Ilex aquifolium*) and yew (*Taxus baccata*),
100 which are the tree species selected for study. Their fruits are sugar-rich red berries
101 (arillated seeds in the case of yew); they present similar morphology, size and coloring
102 and contain either a single seed (hawthorn, yew) or 1-4 seeds (holly). The three tree
103 species ripe in autumn (September to November).

104 The main seed dispersers of these trees are thrushes: blackbird (*Turdus merula*),
105 song thrush (*T. philomelos*), mistle thrush (*T. viscivorus*), fieldfare (*T. pilaris*), redwing
106 (*T. iliacus*) and ring-ouzel (*T. torquatus*). All these thrushes are mostly frugivores
107 during fall and winter, and show a non-selective diet (i.e. the consumption of the
108 fruiting species is proportional to the yearly abundance; García et al. 2013). All thrushes
109 have similar fruit-handling behavior, swallowing the entire fruits after picking them and
110 expelling the intact seeds in their feces. Although some size-based differences in gut
111 retention time are expected between species of thrushes, we assumed these differences
112 to be negligible in terms of effects on seed germination ability. Conversely, each thrush

113 species may vary in their response to landscape structure, a fact that leads to
114 complementary spatial patterns of seed dispersal (Morales et al. 2013, and references
115 within).

116 Previous studies in the same system have revealed that most seeds of the study
117 species are deposited beneath tree canopies, with few reaching uncovered, open areas
118 (García et al. 2005c). Post-dispersal seed predation by rodents (*Apodemus* spp.) varies
119 markedly between microhabitats (under trees >> open areas; García et al. 2005c), and
120 between tree species (*T. baccata* > *I. aquifolium* > *C. monogyna*; García et al. 2005a).
121 Germination of dispersed seeds occurs after 18 months, i.e. in the second spring after
122 seed dispersal, with slight differences between tree species and between microhabitat
123 (Supplementary material Appendix 1, Fig. A3). Seedlings suffer high mortality after
124 emergence due to grazing and trampling by ungulates, but survival increases when
125 seedlings grow under nurse woody plants (García and Obeso 2003, Martínez 2014).

126 ***Study area and field sampling***

127 Field sampling was conducted in the Sierra de Peña Mayor (43°18'00"N, 5°30'29"W,
128 1000 m a.s.l., Asturias, Spain) where secondary forests occur as edging patches next to
129 deciduous forests of beech *Fagus sylvatica* or as variable-sized fragments (from
130 remnant trees to areas of several hectares) interspersed with a historically deforested
131 matrix of pastures and heathland (Herrera et al. 2011). A rectangular plot of 400 m x
132 440 m (17.6 ha) was set up, in order to cover a gradient of forest loss, from dense forest
133 patches to isolated trees scattered through pastures, so the plot was subdivided into 440
134 sampling cells of 20 m x 20 m (Supplementary material Appendix 1, Fig. A1.B).
135 Likewise, a Geographical Information System (GIS, ArcGIS v9.3) was developed in
136 order to estimate the percentage of tree cover per cell (in m²) by incorporating a grid

137 and a digitized forest cover layer. Additionally, in October 2009 and 2010 we estimated,
138 in the field, the position of all individual trees and the fruit crop of each individual tree
139 of the studied fleshy-fruited species within each plot cell (see Supplementary material
140 Appendix 1 for methodological details). For each year, we incorporated the data on fruit
141 production into the GIS platform in order to quantify the number of trees and the total
142 fruit production per cell.

143 From October to February of 2008-2009, 2009-2010 and 2010-2011, we studied
144 the spatially-explicit foraging patterns of each thrush species, quantifying their
145 movements, flight distances and perching habitats, as well as the number of fruits
146 consumed from each tree species. Data collection was based on direct observation
147 sequences of individual birds, made from elevated positions located along the central
148 axis of the plot. During field surveys, we also recorded the presence of individual birds
149 across the plot cells, in order to provide a measure of bird species abundance (see
150 Supplementary material Appendix 1 and references therein).

151 In fall-winter 2009-2010 and 2010-2011 (2009 and 2010 hereafter) we assessed
152 seed deposition by birds in a subset of 220 cells following a checkered pattern
153 (Supplementary material Appendix 1, Fig. A1.C). Within each cell, and in two separate
154 surveys (November and January) of each sampling season, we counted the number of
155 seeds of fleshy-fruited trees found in bird feces in ten sampling stations (open-ground
156 50 cm x 50 cm quadrats) each separated from the others by 2 m (Supplementary
157 material Appendix 1, Fig. A1.C). We assigned each seed sampling station to one of the
158 following five microhabitats depending on the type of fine-scale cover: (a) beneath *C.*
159 *monogyna*, (b) beneath *I. aquifolium*, (c) beneath *T. baccata*, (d) beneath non-fleshy-
160 fruited trees (e.g. *Corylus avellana*) and (e) in the open (i.e. uncovered by tree canopy,
161 e.g. pastures). For each year, in each sampling station, we calculated the number of

162 dispersed seeds per tree species as the sum of seeds found in the two consecutive
163 surveys.

164 From April to late August of 2011 and 2012, in the subset of cells for measuring
165 seed deposition, we recorded the number of emerged seedlings of the tree species under
166 study. For each cell, we established five seedling sampling stations (open-ground 50 cm
167 x 50 cm quadrats), separated from each other by four meters but adjacent to a seed
168 sampling station (Supplementary material Appendix 1, Fig. A1.D). All emerged
169 seedlings were specifically and individually identified, and their survival was monitored
170 monthly throughout the season. We considered a seedling to be established when it
171 survived to the end of the summer, as previous surveys had revealed that the summer
172 period was when seedling mortality was highest (Martínez 2014). The seed dormancy
173 period of all three fleshy-fruited trees lasts 18 months. Thus, we assigned the seedlings
174 emerging in 2010 and in 2011 to the cohorts of seeds dispersed in 2009 and in 2010,
175 respectively. Comprehensive details of field data collection are shown in Supplementary
176 material Appendix 1.

177 *Seed-dispersal interaction matrices at two regeneration stages*

178 Our analytical goal was to compare the structure of plant-seed disperser (tree-bird)
179 networks across two stages of plant regeneration. This requires estimating quantitative
180 matrices of paired tree-bird interactions at seed deposition and seedling recruitment.
181 Thus, interactions should be based on determining which species of bird was likely to
182 have, respectively, deposited a given seed, and have recruited a given seedling. Due to
183 the methodological constraints in obtaining this kind of information in the field (e.g.
184 González-Varo et al. 2014), we opted for an approach based on three principal steps
185 (Fig. 1): (1) estimation of tree-bird and tree-microhabitat matrices of seed deposition

186 (Fig. 1D), based on a mechanistic model of seed dispersal (Fig. 1B); (2) validation of
187 the simulated seed dispersal patterns with field data on the tree-specific seed
188 distributions between microhabitats (Fig. 1D and Fig. 1A); and (3) estimation of the
189 tree-bird matrices of seedling recruitment from the simulated seed deposition matrices
190 (Fig. 1E), taking into account microhabitat-dependent seed fates quantified from field
191 surveys (Fig. 1C).

192 *Seed deposition matrices from a mechanistic model of seed dispersal*

193 We implemented a model that predicts, through stochastic simulations, the deposition of
194 seeds of different species of trees by birds according to mechanistic rules. These rules
195 combined mathematical functions representing the performance of bird species
196 depending on the movement and foraging behavior of each species under a realistic
197 scenario (that of our study site and period). The values of model parameters that
198 determined the shape of the functions varied between species, and were estimated from
199 field data of both the relative abundances of fruits and birds and the foraging activity of
200 bird species. The model used here expands the previous versions developed by Morales
201 and Carlo (2006), Carlo and Morales (2008), and Morales et al. (2013), in the sense that
202 it now predicts seed deposition in the five microhabitats distinguished in our field study
203 (i.e. beneath *C. monogyna*, *I. aquifolium*, *T. baccata*, and non-fleshy-fruited tree
204 species, and in the open). This therefore enabled us to incorporate a quality component
205 to each seed dispersal event, as seed fate is expected to be mostly driven by
206 microhabitat features. A detailed description of the structure of the model and functions
207 fitted is presented in Supplementary material Appendix 2 (see also Morales et al. 2013).

208 Basically, the model simulated individual bird tracks (i.e. the displacement of an
209 individual bird, able to consume fruits and expel seeds while moving) within a grid-

210 based, modeling landscape that replicates the spatial extent and the environmental
211 variability of our 440-cells study plot. Globally, the path of tracks varied depending on
212 bird response to landscape heterogeneity (measured by forest cover and fruit
213 abundance); the outcome of tracks (in terms of fruit consumption and microhabitat-
214 dependent seed deposition) depended on which fruiting species were encountered by
215 birds, gut retention time, and microhabitat-dependent perching probabilities
216 (Supplementary material Appendix 2, Fig. A4). The movement of a bird from one cell
217 to another was predicted by a combination of functions that took into account (Fig. 1A):
218 (a) the distance to the cell where the movement starts, (b) the proportion of forest cover
219 in the destination cell, (c) the number of fruits in the destination cell, and (d) the
220 distance to the edge of the plot (which allowed birds to leave the modeling landscape).
221 The consumption of fruits by a given bird along a track depended on (e) fruit
222 availability in the cell (updated after each track and fruit removal). Gut retention time
223 depended on (f) the body size of each bird species. Finally, the probability of seed
224 deposition in a given microhabitat within a cell depended on the destination perch, a
225 combined function of: (g) the number of fruits of each tree species in that cell, (h) the
226 number of trees of each species in that cell, and (i) the species of the ingested seed (as
227 the probability of deposition beneath a conspecific perching tree has been demonstrated
228 to be higher than beneath other tree species; García et al. 2007). We fitted seed
229 deposition probability in the open microhabitat according to the proportion of forested
230 area within each cell.

231 We obtained each model output (i.e. seed dispersal data) as a spatially-explicit
232 (cell- and microhabitat-based) prediction of seed deposition for each tree species and by
233 each bird species, that is, a multi-specific seed rain across the modeled landscape (Fig.
234 1B). Each model output was the result of a simulation accounting for 5000 bird tracks,

235 and the simulations were replicated 30 times (i.e. 30 independent model outputs), for
236 each of the two year scenarios (2009 and 2010). These year scenarios accounted for the
237 field-based values of fruit availability and abundance of bird species in the respective
238 years. We finally selected the seed deposition output corresponding to a subset of the
239 220 cells of the modeling landscape in equivalent positions to those containing seed
240 deposition and seedling establishment sampling stations in the field (Fig. 1C;
241 Supplementary material Appendix 1, Fig. A1C).

242 The data of each seed deposition output, accounting for tree-bird and tree-
243 microhabitat specific information, were pooled across microhabitats. In this way, we
244 obtained a seed deposition matrix that accounted for the number of seeds of each tree
245 species that were dispersed by each bird species. For each year scenario, we thus
246 obtained 30 matrices of simulated seed deposition (Fig. 1D).

247 *Validation of model-predicted seed deposition*

248 In order to validate the seed deposition patterns predicted by the mechanistic model, we
249 first re-organized the data of seed deposition outputs by pooling the data from all six
250 species of birds. That is, we generated 30 matrices for each study year, with the tree
251 species as rows, the microhabitats as columns and the number of deposited seeds as
252 matrix-cell counts (Fig. 1D). Each year, we then calculated a single simulated seed
253 deposition matrix (the average of the 30 replicates) which was correlated, by means of a
254 Mantel test, with a matrix obtained from seed deposition field data for the
255 corresponding year and using the same tree-microhabitat structure (i.e. the total number
256 of seeds of each tree species collected in each microhabitat; Fig. 1A). We performed the
257 Mantel test using the *ecodist* library in R v. 3.0.2 (R Development Core Team 2013).

258 *Seedling recruitment matrices: incorporating seed fate into simulated seed deposition*

259 Based on the simulated seed deposition raw outputs (that is, those accounting for
260 microhabitat, tree and bird species), we calculated seedling recruitment matrices as the
261 number of established seedlings attributable to each tree and bird species in each
262 microhabitat (Fig. 1E). For each year (i.e. seeds corresponding to the same yearly
263 fruiting cohorts), we multiplied each simulated seed deposition output by two matrices
264 of transition probabilities: a) a *seedling emergence rate* (i.e. the proportion of deposited
265 seeds from which a seedling emerged after an 18-months post-dispersal period), and b)
266 a *seedling survival rate* (i.e. the proportion of emerged seedlings which survived to the
267 end of the summer season). All transition probabilities were estimated from field data
268 for each tree species, microhabitat and year (seed cohort). Namely, seedling emergence
269 of a given tree species in a given microhabitat was calculated by matching the total
270 number of emerged seedlings of that species, in the sampling stations of that
271 microhabitat, with the total number of seeds of the corresponding cohort deposited in
272 the adjacent seed sampling stations (Supplementary material Appendix 1, Fig. A1.C).
273 Seedling survival was also calculated in each microhabitat, for each species and year, by
274 dividing the total number of established seedlings in the sampling stations of a given
275 microhabitat by the total number of emerged seedlings in those stations.

276 Similar to the simulated seed deposition matrices, we further re-organized
277 seedling recruitment matrices by pooling the number of established seedlings across
278 microhabitats in order to produce matrices with tree species as rows, birds species as
279 columns, and the number of established seedlings as cell counts, for each year (Fig. 1E).

280 ***Network analyses***

281 A quantitative network approach was used to evaluate the structure of interactions
282 between fleshy-fruited trees and frugivorous birds, considering separately the

283 regeneration stages of seed deposition and seedling recruitment and two cohorts (2009
284 and 2010; Fig. 1). For each cohort, we applied network analyses to the 30 replicates of
285 our simulated seed deposition and seed recruitment matrices.

286 As would be suggested by previous conceptual models (Carlo & Yang 2011;
287 Schleuning et al. 2015), we were expecting that incorporating seed fate into plant-
288 frugivore networks would lead to changes in the relative frequencies (interaction
289 weights) and the number of paired interactions (links) within the network. In view of
290 this, we exclusively focused on two complementary metrics representing different
291 aspects of the diversity of interactions in the global network: *interaction evenness* and
292 *linkage density*. Interaction evenness is calculated from the Shannon's evenness index.
293 It is a measure of the heterogeneity of interaction frequencies in *the whole network* (e.g.
294 a more heterogeneous network is expected when few strong tree-bird interactions
295 dominate seed deposition or seedling recruitment). In other words, it provides additional
296 information about the relative allocation of the contributions of all the frugivores for
297 seed dispersal and seedling recruitment. It ranges from 0 (uneven networks) to 1
298 (uniform network) and the change in this metric would reflect changes in the
299 distribution of interaction weights in the whole network, even with no modifications in
300 the number of interacting species. Linkage density is a measure of the mean number of
301 links per species, weighted by the number of interactions. Thus, it reflects the average
302 richness of links per species at the global network level, and its variability quantifies
303 interaction gains or losses. In weighted networks, changes in this metric also represent
304 the variability in the distribution of interaction weights *within specific species*. For more
305 detailed definitions of the parameters used see Dormann et al. (2009).

306 These two topological parameters were calculated using the *networklevel*
307 function from the *bipartite* package (version 2.05, Dormann, et al. 2009). Likewise,

308 network graphs were represented with the *plotweb* function. Finally, we compared the
309 values of network metrics between years for both seed deposition and recruitment by
310 means of two sample t-tests, and between regeneration stages from a given cohort, by
311 means of paired t-tests. All statistical analyses were performed in the R statistical
312 software version 3.0.2 (R Development Core Team 2013).

313

314 **RESULTS**

315 *Overview of field results*

316 Field sampling evidenced **strong inter-annual variability** in the total abundance of fruits,
317 seeds and seedlings of tree species from 2009 to 2010, **as well as of the species of birds**
318 (Fig. 2). All six species of birds were observed in both study years, but *T. pilaris* and *T.*
319 *torquatus* accounted for less than 2% of bird observations in each year. However, inter-
320 annual variability was found for the remaining bird species. Namely, *T. iliacus* was the
321 dominant bird in 2009, while *T. philomelos* showed the highest relative abundance in
322 2010 (Fig. 2A). *T. merula* and *T. viscivorus* always showed intermediate values of
323 relative abundance.

324 **The total abundance of fleshy fruits increased from 2009 to 2010 (Fig.2B).**

325 While in 2009 *I. aquifolium* was the dominant species with almost 84% of the total fruit
326 crop, in 2010 it was *C. monogyna* with 65%. Moreover, *T. baccata* accounted for less
327 than 10% of fruits in both years. Hence, the fruiting landscape changed between years
328 (Supplementary material Appendix 1, Fig. A2) as a result of the differences in the
329 relative abundance of species between years and their spatial distribution.

330

331 As regards seed deposition, *I. aquifolium* was always the most abundant species,
332 even in 2010, when the higher number of seeds per fruit partially compensated for its
333 lower fruit production, compared with *C. monogyna* (Fig. 2C).

334 Concerning dispersed seeds across microhabitats, both years more than 70% of *I.*
335 *aquifolium* seeds were deposited beneath conspecific trees, whereas more than 45% of
336 *C. monogyna* seeds were dropped beneath heterospecific, fleshy-fruited trees
337 (Supplementary material Appendix 3, Table A3). For *T. baccata*, conspecific canopy
338 received the largest proportion of seeds. The percentage of seeds found in open areas
339 was always lower than 12%, with *C. monogyna* being the species with most seeds
340 reaching this microhabitat.

341 The relative abundance of emerged and surviving seedlings was always higher
342 for *I. aquifolium*, most notably in the 2009 cohort (Fig. 2D and Fig. 2E). Nevertheless,
343 *C. monogyna* showed higher relative abundances of emerged and surviving seedlings
344 than expected from its relative abundances at seed deposition. Indeed, in both years the
345 latter was the species with the highest *seedling emergence rates* in all microhabitats,
346 especially in open areas (Supplementary material Appendix 3, Table A4). *Seedling*
347 *survival rates* were lower for *C. monogyna* than for *I. aquifolium* or *T. baccata* beneath
348 cover microhabitats, but the reverse occurred in open areas.

349 ***Seed deposition model prediction and validation***

350 Simulations showed that seeds of all three tree species were mainly dispersed beneath
351 their conspecifics, and the percentage of seeds found in open areas was always lower
352 than 12% for all tree species and years with *C. monogyna* being, comparatively, the
353 species with the highest numbers of seeds arriving in this kind of microhabitat
354 (Supplementary material Appendix 3, Table A6). In both years, these simulation results

355 agreed with field data, as suggested by the positive and significant correlations between
356 the observed and the simulated proportion of each species of seeds found in each
357 microhabitat (Mantel test: $r \geq 0.889$, $p \leq 0.015$, for both years; Supplementary material
358 Appendix 3, Tables A3 and A6). Our mechanistic model was, thus, able to explain a
359 high proportion of the observed variability in seed dispersal.

360 Most bird species (particularly *T. iliacus*) dispersed the majority of the simulated
361 seeds beneath canopies of fleshy-fruited tree species, but *T. viscivorus* and *T. pilaris*
362 displaced a comparatively higher proportion of seeds into open areas (Supplementary
363 material Appendix 3, Table A8). These differences between bird species were
364 accentuated in the transition from seed deposition to seedling recruitment
365 (Supplementary material Appendix 3, Table A9).

366 ***Interaction networks for different regeneration stages and years***

367 Bipartite graphs revealed that the interaction frequencies of the six birds and the three
368 trees changed between regeneration stages and years. In 2009, *T. iliacus*, together with
369 *T. philomelos* and *T. merula*, accounted for 93% of seed deposition interactions and
370 89% of seedling recruitment, whereas, it was *T. philomelos* and *T. merula* that
371 dominated both networks in 2010. With respect to trees, the interaction frequency of *C.*
372 *monogyna* increased from seed deposition to recruitment networks, especially in 2009
373 (Fig. 3).

374 Regarding the network metrics, we found a significant increase in interaction
375 evenness from seed deposition to seedling recruitment for both cohorts (Fig. 4), in 2009
376 (paired-t= 21.49; $p < 0.0001$) and in 2010 (paired-t= 3.37; $p = 0.002$). That is, in both
377 cases the homogeneity of interaction weights within the whole network was higher at
378 the seedling recruitment stage than at the seed deposition one, especially in the cohort of

379 2009. Similarly, linkage density increased from seed deposition to the recruitment stage
380 in the 2009 cohort (paired-t= 19.43; p<0.0001). This latter structural change was
381 probably related to a modification in the distribution of the interaction weights when
382 looking at the specific species, namely the decrease of dominance of *I. aquifolium*
383 within the main bird species (*T. iliacus*, *T. philomelos*, Fig. 3). However, we found an
384 opposite trend for the 2010 cohort, with a decrease in the linkage density across
385 regeneration stages (paired-t= -8.66; p<0.0001). The increase in the dominant role of *C.*
386 *monogyna* from seed deposition to recruitment and, more importantly, the loss of
387 interactions within the networks, such as the ones between three species of birds when
388 recruiting *T. baccata* probably underpinned the decrease in linkage density (Fig. 3).

389 Inter-annual differences between networks corresponding to a given
390 regeneration stage were also found (Fig. 4). The distribution of interactions for seed
391 deposition networks was more homogeneous in 2010 than in 2009 (interaction
392 evenness; t= 4.78; p<0.0001), apparently due to the decreased dominance of *I.*
393 *aquifolium* (Fig. 3). At the same time, and probably derived from the increased
394 weighting of *T. philomelos* and *C. monogyna*, the whole recruitment networks presented
395 the opposite trend, being less even in 2010 than in 2009 (t= -12.46; p<0.0001).
396 However, the values of linkage density decreased between cohorts for both regeneration
397 stages (seed deposition: t= -5.75; p<0.0001; recruitment: t= -18.71; p<0.0001), also
398 probably due to the increase in the dominance of a few birds within the main tree
399 species (*I. aquifolium* and *C. monogyna*).

400

401 **DISCUSSION**

402 Plant-seed disperser networks have been widely explored in previous studies (e.g.
403 Donatti et al. 2011, Mello et al. 2014) in order to identify the topological generalities of
404 these ecological assemblages as well as the consequences of these generalities in terms
405 of stability or evolutionary potential. These studies have usually represented the
406 complexity of plant-frugivore interactions only at the beginning of the plant
407 regeneration process, being blind to the final functional effect of these interactions
408 (Carlo & Yang 2011). In this study we overcome this partial view of interaction
409 diversity in plant-animal assemblages, by incorporating seed fate into simulated plant-
410 seed disperser networks. By using a mechanistic model parameterized with field data,
411 we were able to estimate frugivore-specific seed deposition in different microhabitats.
412 Seed dispersal interactions were later translated into interactions between frugivores and
413 plants at the seedling stage by accounting for field-measured, microhabitat-dependent
414 recruitment expectancies. Overall, we show that the diversity of interactions may
415 increase across plant regeneration stages, and also change between successive plant
416 cohorts.

417

418 *Variability in interaction diversity across plant regeneration stages*

419 Here, we took into account the transition between plant regeneration stages, seen as the
420 result of filtering agents (e.g. frugivores, seed predators, abiotic factors causing seedling
421 mortality; Zamora and Matías 2014) operating on successive demographic processes
422 (fruit removal and seed dispersal, seedling establishment; Wang and Smith 2002). We
423 assumed that these filters may modify the global distribution of interaction frequencies
424 between plant and bird species from the stage of seed dispersal to that of seedling

425 recruitment, and thus that these distribution changes are well represented by network
426 metrics related to interaction diversity (Schleuning et al. 2015).

427 We first detected changes in the dominance of interactions, as reflected by the
428 increase in interaction evenness, from seed dispersal to recruitment (most notably in the
429 cohort of 2009). Thus, tree and bird species made a more even contribution to the whole
430 interaction network after accounting for post-dispersal fate. A negative correlation
431 between the quantitative and qualitative roles of seed dispersers (with the most frequent
432 disperser having the lowest quality and *vice versa*) could explain such an increase in
433 interaction evenness (Schleuning et al. 2015). However, no strong differences between
434 species of thrushes were expected in seed gut treatment, and no relationship between the
435 abundance of the different thrushes and their contribution to the seed rain was apparent
436 (Fig. 2; Supplementary material Appendix 3, Table A8). We thus need to search for
437 alternative arguments to explain changes of evenness. In this sense, these modifications
438 accord with *C. monogyna* having a stronger, and far more equitable role in the
439 networks, compared to *I. aquifolium*. This probably derived from the higher emergence
440 rates of *C. monogyna* compared to the other trees (Supplementary material Appendix 3,
441 Table A4), and as a consequence of its generally lower seed predation rate (due to its
442 thicker seed coat; García et al. 2005a). These differences in emergence may be
443 accentuated by subtle differences between trees in their spatial patterns of seed
444 dispersal. Namely, compared to the other trees, *C. monogyna* showed a higher
445 proportion of seeds reaching open areas (where seed predation is lower and germination
446 slightly higher; García et al. 2005c), as well as a higher proportion of seeds dispersed
447 below heterospecific canopies (where co-deposition with other species further decreases
448 the predation rate; García et al. 2007).

449 Concerning linkage density, a decrease in the value of this metric is expected
450 when demographic filtering leads to the disappearance of some links from the network
451 of seed deposition (e.g. when plant species reduce their coteries of dispersers, thereby
452 losing links with bad-quality dispersers; e.g. Carlo and Yang2011). In our case,
453 microhabitat differences in seed fate, and bird differences in seed deposition patterns,
454 seemed to determine a weak-to-moderate gradient in seed disperser quality, with
455 probably weak effects on the loss of links. Nevertheless, we would expect a decrease in
456 linkage density along the demographic process if some links could be lost just owing to
457 sampling effects, when all the seeds of rare plants, dispersed by rare frugivores,
458 disappear after heavy post-dispersal losses. This is what we found for the 2010 cohort, a
459 decrease in the number of links between *T. baccata* and the species of birds responsible
460 for its recruitment (Fig. 3). The high predation rate suffered by seeds of *T. baccata* in
461 the Cantabrian range (García et al. 2005a, 2007), and the concomitant low establishment
462 probability of this species, may also underpin the loss of interactions concerning this
463 tree across regeneration stages. On the other hand, as the number of links could not
464 become larger from seed dispersal to recruitment, higher values found for the 2009
465 cohort reveals that these changes were due to the relative weight of each plant species
466 within each frugivore species (for example as a consequence of the increase in the
467 relative role of *C. monogyna* in the recruitment network).

468

469 ***Inter-annual variability in seed deposition and recruitment networks***

470 Our comparison of two plant cohorts evidenced strong differences in interaction
471 frequencies in terms of the distribution across tree and bird species, as well as with
472 regards to the global structure of networks. Changes in interaction frequencies at the

473 seed deposition stage seemed to mirror between-year variation in the relative
474 abundances of both fruits and birds. As for birds, most of the inter-annual variability
475 was accounted for by the opposing trends of *T. iliacus* and *T. philomelos*. Variations in
476 the number of migrant individuals reaching and wintering in the Cantabrian Range each
477 year probably supported these differences (Tellería et al. 2014). As *T. iliacus* decreased
478 in abundance from 2009 to 2010, the seed dispersal and recruitment networks were
479 dominated by *T. philomelos*, with a concomitant decrease in linkage density. With
480 respect to trees, the variability in fruit crop composition provoked by the alternating
481 masting events of *I. aquifolium* and *C. monogyna* cascaded into strong changes in the
482 relative dominance of each species, affecting interaction evenness. In sum, our study
483 evidences that the functional effect of seed dispersal networks depends on the, typically
484 strong, inter-annual dynamism of the fruit-frugivore interaction (see also Carnicer et al.
485 2009).

486 Post-dispersal processes may, however, buffer the weight of relative abundances
487 at the seed dispersal stage when driving inter-annual differences in recruitment
488 networks. For example, for the 2010 cohort, the proportion of seeds in the open and
489 beneath non-fleshy trees (microhabitats allowing higher rates of seedling emergence)
490 was comparatively higher, irrespective of the tree and the bird species. This was
491 probably the result of all birds using landscape sectors rich in these types of
492 microhabitats more frequently in 2010 in response to the fruit crop being more widely
493 distributed across the whole study plot (Supplementary material Appendix 1, Fig. A2;
494 Martínez and García, 2014).

495

496 **CONCLUDING REMARKS**

497 We show here that the interaction diversity in plant-seed disperser networks increases
498 when considering the functional effect of birds on plants. The process of demographic
499 filtering on plants could neutrally provoke these changes by itself, as the random loss of
500 plant propagules would make those depending on rare interactions become even rarer.
501 Nonetheless, we pinpoint two deterministic forces equalizing the interactions across
502 plant regeneration: disperser quality, here dependent on how the spatial pattern of seed
503 deposition matches that of seed fate; and plant species traits, as each species may make
504 their recruitment more dependent on specific traits (here, for example, seed hardness
505 driving differences in seed predation) than on the deposition microhabitat imposed by
506 dispersers. Interactions between disperser quality and plant traits are, nevertheless,
507 possible, as, on the one hand, a seed not favored for frugivore removal may still recruit
508 if deposited in a particular microhabitat (e.g. García et al. 2007), and, on the other hand,
509 the effect of some plant traits may differentially emerge depending on the microhabitat
510 (e.g. seed hardness becoming innocuous when there are very few seed predators; García
511 et al. 2005c). In sum, this work strongly recommends the development of an integrative
512 framework to predict the balanced and interactive effects of plant and animal traits in
513 the functional outcome of plant-animal mutualistic networks (Schleuning et al. 2015).
514 Further studies should corroborate the present results in species-rich plant-seed
515 disperser assemblages, such as tropical ones (e.g. Donatti et al. 2011), by incorporating
516 the demographic data needed to assign specific fates to the seeds of different plants
517 dispersed by different animals.

518

519 **Acknowledgements:** We thank J. Rodríguez, C. Guardado and R. Pérez for technical
520 support during fieldwork. J. Fründ and J.M. Morales for statistical advice and R.
521 Lendrum for linguistic review. Dries Bonte and two anonymous referees provided

522 useful suggestions to improve an early version of the manuscript. This research was
523 supported by the Spanish National Program of Research and Development (MICINN
524 CGL2011-28430 grant to DG) and the FPI Program - European Social Fund (BES2009-
525 25093 and BES2012-052863 grants to DM and ID, respectively). Fieldwork was
526 conducted according to Spanish environmental legislation and with the permission of
527 the Regional Government of Asturias.

528

529 **REFERENCES**

530 Albrecht, J. et al. 2013. Logging and forest edges reduce redundancy in plant-frugivore
531 networks in an old-growth European forest. - *J. Ecol.* 101: 990–999.

532 Bascompte, J. and Jordano, P. 2007. Plant-animal mutualistic networks: The
533 architecture of biodiversity. - *Annu. Rev. Ecol. Evol. Syst.* 38: 567–593.

534 Blüthgen, N. and Klein, A. M. 2011. Functional complementarity and specialisation: the
535 role of biodiversity in plant–pollinator interactions. - *Basic Appl. Ecol.* 12: 282–
536 291.

537 Carlo, T. and Morales, J. 2008. Inequalities in fruit-removal and seed dispersal:
538 consequences of bird behaviour, neighbourhood density and landscape
539 aggregation. - *J. Ecol.* 96: 609–618.

540 Carlo, T. A. and Yang, S. 2011. From frugivory to seed dispersal networks: challenges
541 and opportunities of a new paradigm. - *Acta Oecol.* 27: 619–624.

542 Carnicer, J. et al. 2009. The temporal dynamics of resource use by frugivorous birds: a
543 network approach. - *Ecology* 90: 1958–1970.

544 Chama, L. et al. 2013. Habitat Characteristics of Forest Fragments Determine
545 Specialisation of Plant-Frugivore Networks in a Mosaic Forest Landscape. - PLoS
546 ONE 8: e54956.

547 Donatti, C. I. et al. 2011. Analysis of a hyper-diverse seed dispersal network:
548 modularity and underlying mechanisms. - Ecol. Lett. 14: 773–781.

549 Dormann, C. F. et al. 2009. Indices, graphs and null models: analyzing bipartite
550 ecological networks. - Open Ecol. J. 2: 7-24.

551 García, D. and Obeso J.R. 2003. Facilitation by herbivore-mediated nurse plants in a
552 threatened tree *Taxus baccata*: local effects and landscape level consistency. -
553 Ecography 26: 739-750.

554 García, D. et al. 2005a. Rodent seed predation promotes differential recruitment among
555 bird-dispersed trees in temperate secondary forests. - Oecologia 144: 435–46.

556 García, D. et al. 2005b. Fragmentation patterns and protection of montane forest in the
557 Cantabrian range (NW Spain). - Forest Ecol. Manag. 208: 29–43.

558 García, D. et al. 2005c. Spatial concordance between seed rain and seedling
559 establishment in bird-dispersed trees: does scale matter? - J. Ecol. 93: 693–704.

560 García, D. et al. 2007. Seed transfer among bird-dispersed trees and its consequences
561 for post-dispersal seed fate. - Basic Appl. Ecol. 8: 533–543.

562 García, D. et al. 2013. Functional heterogeneity in a plant-frugivore assemblage
563 enhances seed dispersal resilience to habitat loss. - Ecography 36: 197–208.

- 564 González-Castro, A. et al. 2014. Comparing seed dispersal effectiveness by frugivores
565 at the community level. - Ecology 96: 808–818.
- 566 González-Varo, J. P. et al. 2014. Who dispersed the seeds? The use of DNA barcoding
567 in frugivory and seed dispersal studies. - Methods Ecol. Evol. 5: 806–814.
- 568 Herrera J.M. et al. 2011. Differential effects of fruit availability and habitat cover for
569 frugivore-mediated seed dispersal in a heterogeneous landscape. - J. Ecol. 99:1100-
570 1107.
- 571 Martínez, D. 2014. Seed dispersal and forest recolonization in a fragmented landscape.
572 Looking for the footprint of thrushes (*Turdus* spp.) beyond the forest. PhD thesis,
573 University of Oviedo. Oviedo.
- 574 Martínez, D. and García, D. 2015. Changes in the fruiting landscape relax restrictions
575 on endozoochorous tree dispersal into deforested lands. - Appl. Veg. Sci. 18: 197–
576 208.
- 577 Mello, M. A. R., et al. 2015. Keystone species in seed dispersal networks are mainly
578 determined by dietary specialization. Oikos 124: 1031–1039.
- 579 Morales, J. M. and Carlo, T. A. 2006. The effects of plant distribution and frugivore
580 density on the scale and shape of dispersal kernels. - Ecology 87: 1489–96.
- 581 Morales, J. M. et al. 2013. Frugivore behavioural details matter for seed dispersal: A
582 multi-species model for Cantabrian thrushes and trees. - PLoS One 8: e65216.

583 Plein, M. et al. 2013. Constant properties of plant-frugivore networks despite
584 fluctuations in fruit and bird communities in space and time. - *Ecology* 94: 1296–
585 1306.

586 R Development Core Team 2013. *R: a Language and Environment for Statistical*
587 *Computing*. R Foundation for Statistical Computing, Vienna.

588 Schleuning, M. et al. 2012. Specialization of mutualistic interaction networks decreases
589 toward tropical latitudes. - *Curr. Biol.* 22: 1925–1931.

590 Schleuning, M. et al. 2015. Predicting ecosystem functions from biodiversity and
591 mutualistic networks: an extension of trait-based concepts to plant–animal
592 interactions. - *Ecography* 38:380-392.

593 Schupp, E. W. et al. 2010. Seed dispersal effectiveness revisited: a conceptual review. -
594 *New Phytol.* 188: 333–353.

595 Tellería, J. L. et al. 2014. Species abundance and migratory status affects large-scale
596 fruit tracking in thrushes (*Turdus* spp.). - *J. Ornithol.* 155: 157–164.

597 Thompson, R. M. et al. 2012. Food webs: reconciling the structure and function of
598 biodiversity. - *Trends Ecol. Evol.* 27: 689–697.

599 Tylianakis, J. M. et al. 2010. Conservation of species interaction networks. - *Biol.*
600 *Conserv.* 143: 2270–2279.

601 Vázquez, D. P. et al. 2007. Species abundance and asymmetric interaction strength in
602 ecological networks. - *Oikos* 116: 1120–1127.

- 603 Vázquez, D. P. et al. 2012. The strength of plant-pollinator interactions. - Ecology 93:
604 719–725.
- 605 Wang, B. C. and Smith, T. B. 2002. Closing the seed dispersal loop. - Trends Ecol.
606 Evol. 17: 379–386.
- 607 Xiao, Z. et al. 2015. Seed size and number make contrasting predictions on seed
608 survival and dispersal dynamics: A case study from oil tea *Camellia oleifera*. -
609 Forest Ecol. Manag. 343: 1–8.
- 610 Zamora, R. and Matías, L. 2014. Seed dispersers, seed predators, and browsers act
611 synergistically as biotic filters in a mosaic landscape. - PLoS One 9: e107385.
- 612
- 613 Supplementary material (Appendix oik.XXXXXX at
614 <www.oikosjournal.org/readers/appendix>). Appendix 1–3.

615 **Figure captions**

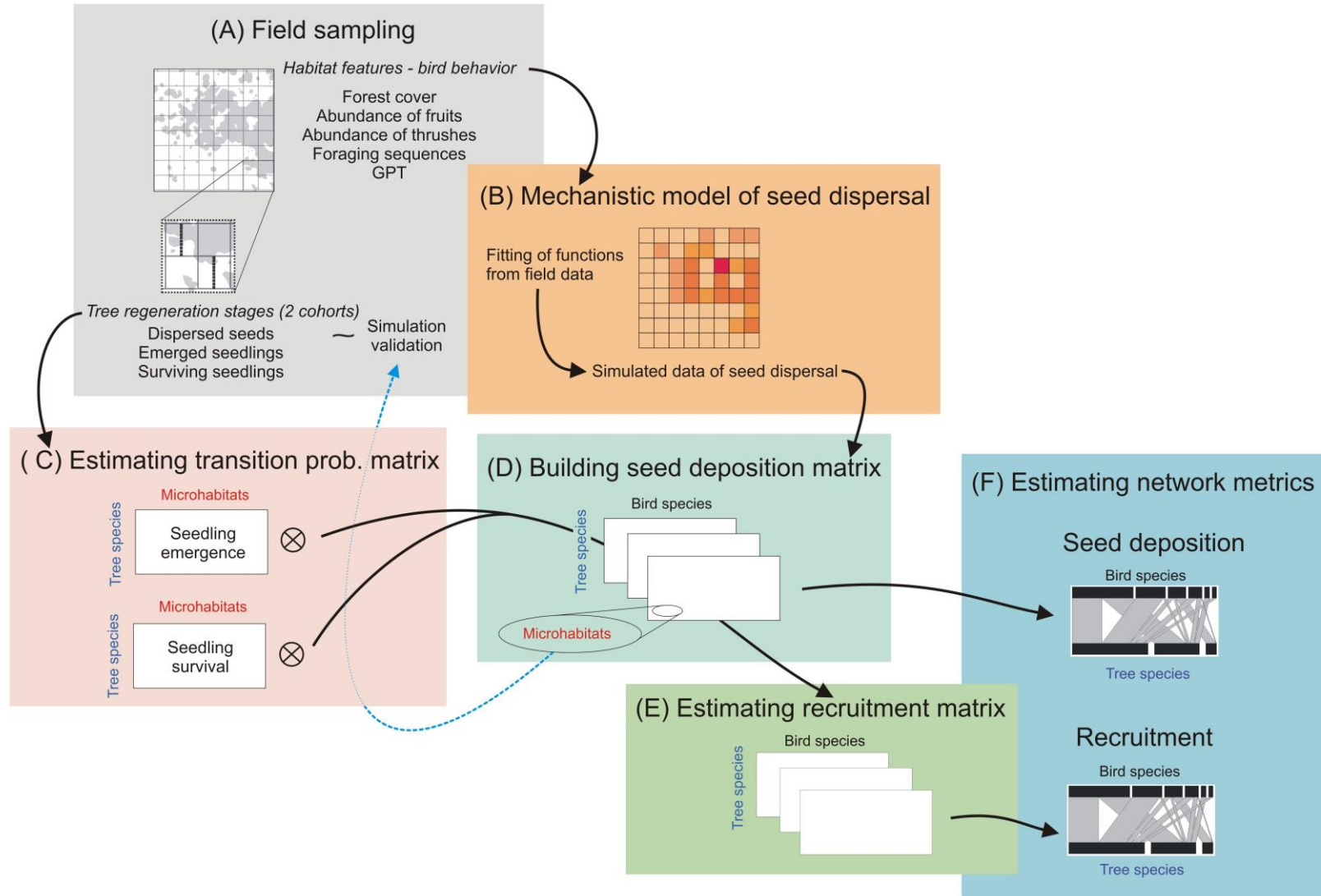
616 **Figure 1.** Flow diagram representing the overall procedure to obtain networks of the
617 two plant regeneration stages (i.e. seed deposition and seedling recruitment). Each step
618 is represented by different colors and how the information is used across these steps is
619 specified by black arrows (but see the blue dashed line arrow for the model validation
620 procedure). (A) Field data sampling took place during two years (2009-2010 and 2010-
621 2011) representing two plant cohorts. (B) This information was used to parameterize the
622 movement and foraging behavior rules of a spatially-explicit mechanistic model. (C)
623 Empirical data on tree regeneration stages was used to estimate transition probability
624 matrices of seedling emergence and seedling survival with different microhabitats as
625 columns (in red) and tree species as rows (in blue). (D) We estimated the seed
626 deposition matrices given the simulated data of the number of seeds dispersed of each
627 plant species (as rows, in blue) by each bird species (as columns, in black) in each of the
628 five microhabitats (in red), coming from the mechanistic model after 30 replicates.
629 Afterwards, we built the seed deposition matrices by pooling the seeds of each plant
630 species dispersed by each bird species across microhabitats. For each cohort, the mean
631 simulated seed deposition matrix was validated with those obtained from field data each
632 year (dashed line arrow). (E) Then, seed deposition matrices were transformed into
633 seedling recruitment by taking into account tree- and microhabitat-specific seed fate
634 (i.e. emergence and survival probabilities) estimated from field sampling and pooling
635 again the seeds of each plant species across microhabitats so as to get the recruitment
636 matrices with bird species as columns (in black), and tree species as rows (in blue). (F)
637 Finally, we compared the structure of seed deposition and seedling recruitment
638 networks by calculating global metrics.

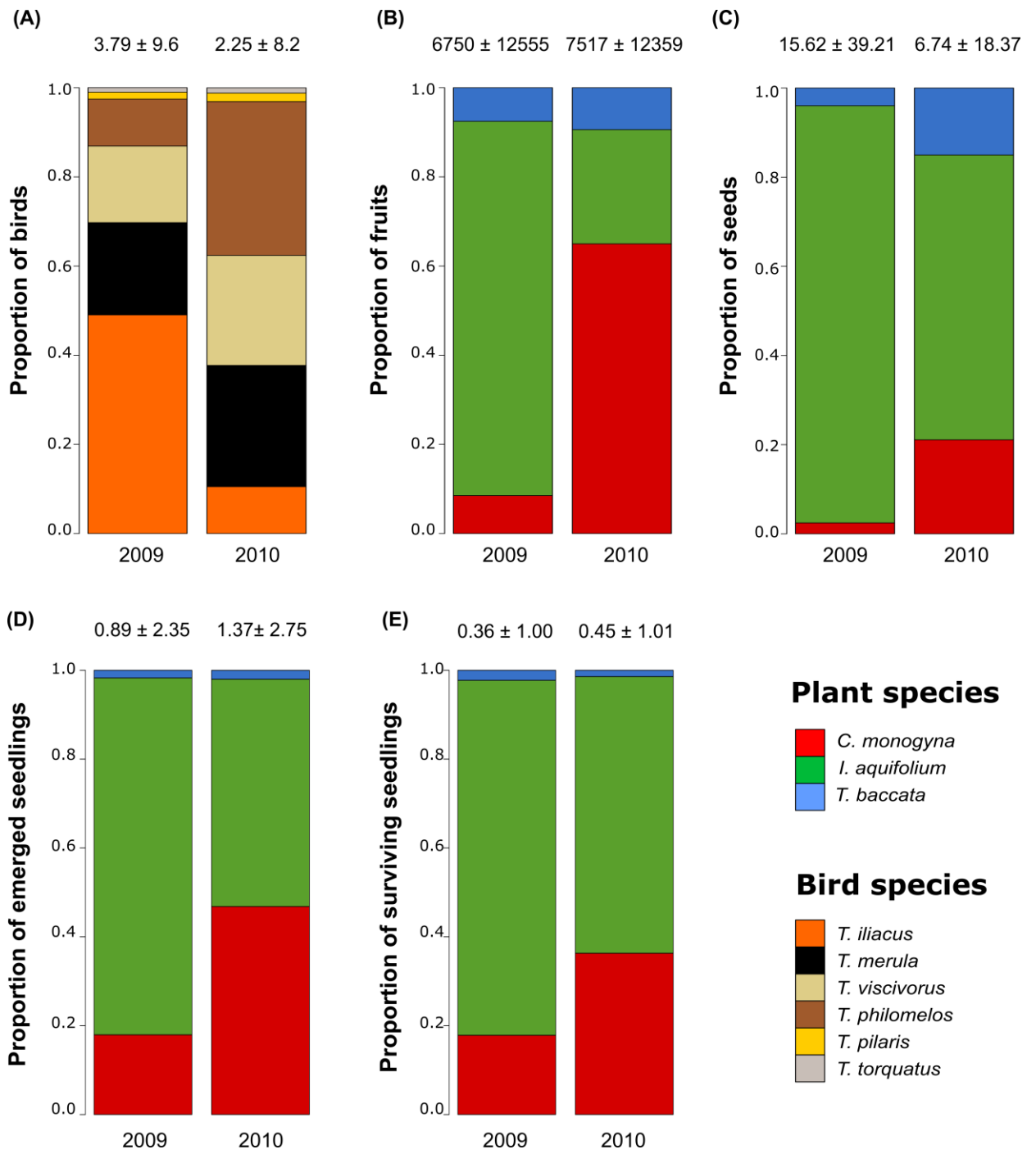
639 **Figure 2.** (A) Abundances of bird species relative to total bird abundance, (B)
640 proportions of fruits of each tree species, (C) proportion of seeds of each tree species
641 with respect to the total seed rain collected, (D) proportions of emerged seedlings of
642 each tree species, and (E) proportions of surviving seedlings of each tree species, for
643 two years (plant demographic cohorts). Above the bar of each year: mean \pm standard
644 deviation of (A) fruits per cell; (B) birds per 10 h per cell; (C) seeds per sampling
645 station per cell; (D) emerged seedlings per sampling station per cell; and (E) surviving
646 seedlings per sampling station per cell (A-B: N=440 cells; C-E: N=220 cells).

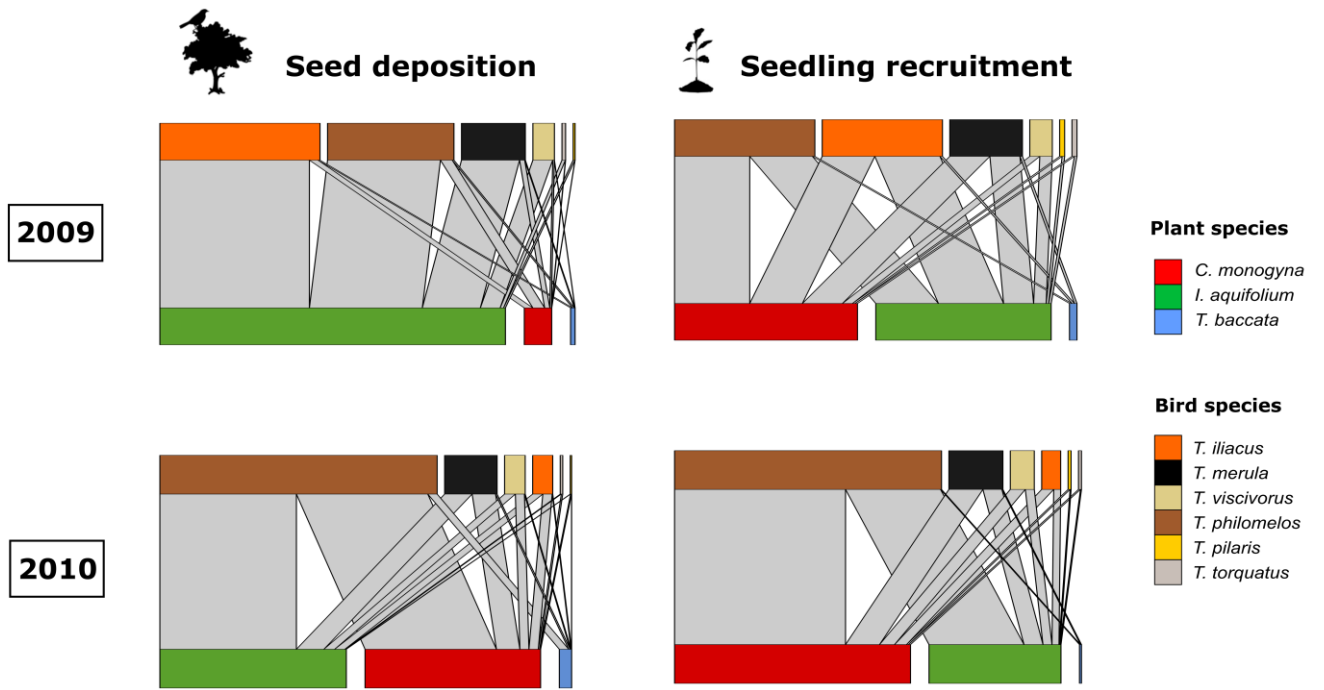
647 **Figure 3.** Bipartite graphs representing the interaction networks between species of
648 birds and trees at different tree regeneration stages (left: seed deposition; right: seedling
649 recruitment) and years (2009 and 2010 seed-to-seedling cohorts). They represent the
650 proportion of dispersed seeds and recruited seedlings of fleshy-fruited trees (bottom
651 rows), those dispersed or recruited by birds (top rows) and the proportion of dispersed
652 seeds or recruited seedlings per tree and bird (gray links).

653 **Figure 4.** Boxplots representing the distribution of values of two network metrics
654 (interaction evenness and linkage density) corresponding to interaction matrices (N =
655 30) for different tree regeneration stages (seed deposition, seedling recruitment) and
656 cohorts (2009, 2010). Bottom and top of boxes correspond to lower and upper quartiles
657 respectively; notches indicate the 95% confidence intervals around the median (black
658 band). Note that the Y-axis varies between indices.

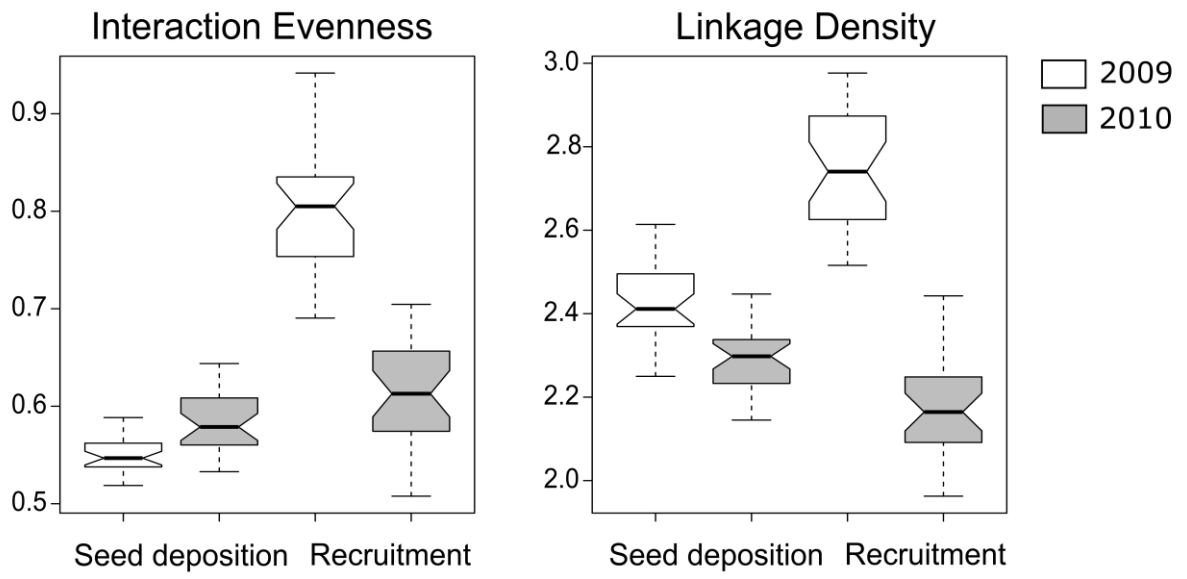
659 **Figure 1**







665 **Figure 4**



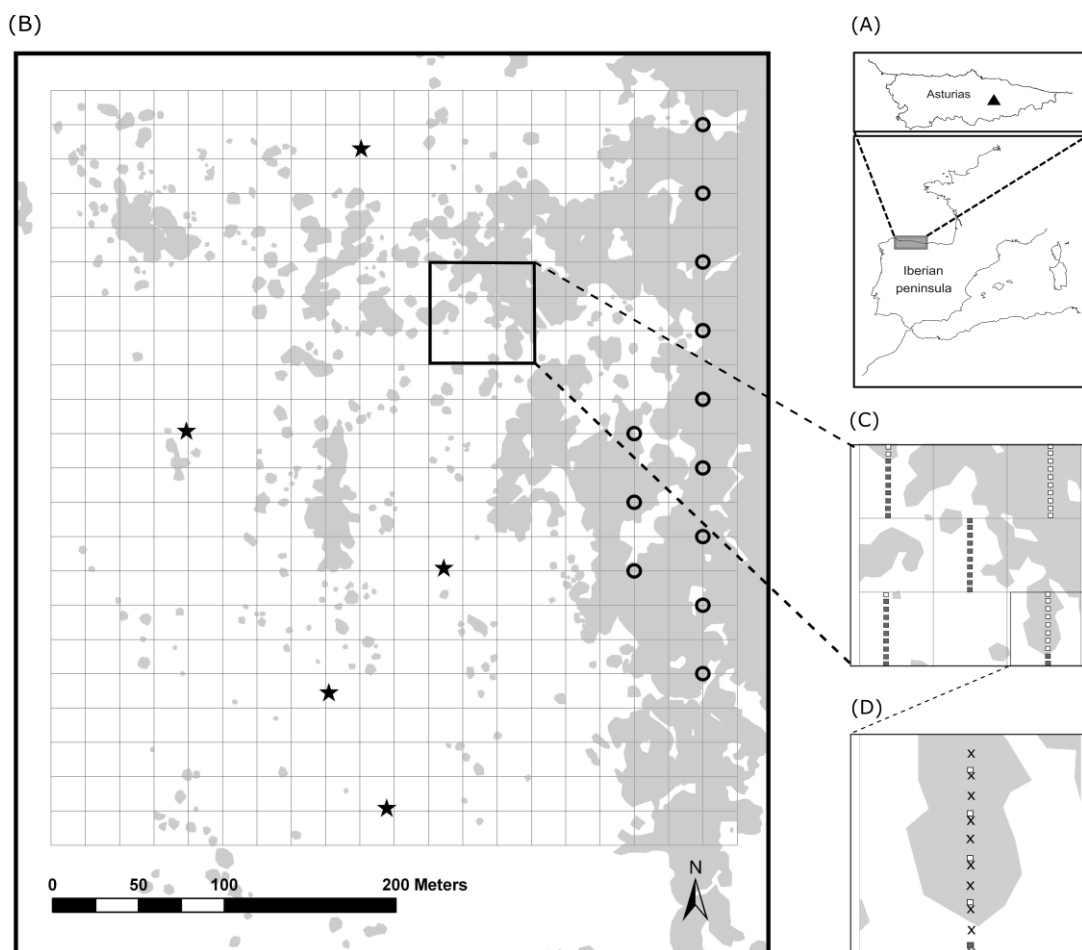
666

1 SUPPLEMENTARY MATERIAL

2 **Appendix 1 – Detailed methodology and additional results of field study**

3 *1. Study plot, forest cover and fruit abundance*

4 Field study was conducted at the Sierra de Peña Mayor (43°18'00''N, 5°30'29''W,
5 1000 m a.s.l., Asturias, northern Iberian Peninsula; Supplementary Material Appendix 1
6 Fig. A1.A). Field sampling was carried out in a rectangular plot of 400 m x 440 m (17.6
7 ha), chosen to represent a gradient of forest loss, from dense forest patches to pastures
8 with scattered trees. Our plot was subdivided into 440 sampling cells of 20 m x 20 m.
9 This combination of sampling extent and grain is known to adequately represent the
10 spatial scale at which tree regeneration processes operate (from frugivory by birds to
11 seedling survival) (García et al. 2013).



12

13 **Figure A1** (A) Location of the study site. (B) Scheme of the study plot representing forest cover
14 (gray area) in the 440, 20 m x 20 m sampling cells, as well as the vantage and point-count
15 positions for bird observation (black stars and circles, respectively). (C) A detail of the
16 distribution of seed-rain sampling stations within a subset of cells, which followed a checkered
17 pattern. (D) Detail of a cell showing the distribution of seedling sampling stations located
18 adjacent to seed rain stations (represented by crosses).

19

20 In 2009 we developed a Geographical Information System (GIS hereafter; ArcGIS v9.3)
21 based on a recent 1:5000-scale orthophotomap image of the study plot to estimate the
22 percentage of cover per cell (in m²) after a digitized forest cover layer and the grid of
23 the 440 sampling cells were integrated. We assumed that inter-annual variability in
24 forest cover was insignificant. Additionally, in 2008, 2009, 2010 and 2011, we assessed
25 the position of all individual trees and the fruit crop of each individual fleshy-fruited
26 tree within each cell in order to incorporate data on fruit production into the GIS
27 platform. For this purpose, we visually assigned the standing crop of each individual
28 tree of any fleshy-fruited species by means of a semi-quantitative Fruiting Abundance
29 Index (FAI) using a semi-logarithmic scale (considering six intervals: 0 = without fruits;
30 1 = 1-10 fruits; 2 = 11-100; 3 = 101-1,000; 4 = 1,001-10,000; 5 > 10,001; Saracco et al.
31 2005). For each sampling year, we thus included in our GIS platform all data on
32 location, species and FAI of each individual tree. Finally, we calculated the number of
33 trees, as well as the total fruit production per year, per cell, as the sum of the crops of all
34 fruiting trees, both for each individual tree species and for all tree species together. Crop
35 size was extrapolated from FAI ranks following an allometric equation (crop size = 1.77
36 $\times e^{1.92FAI}$; $R^2 = 0.080$; $n = 136$ trees, Herrera et al. 2011).

37 Fruiting tree species showed strong inter-annual variation in fruit crop. For
38 instance, in 2009, it was proportionally higher for *I. aquifolium* than for *C. monogyna*,

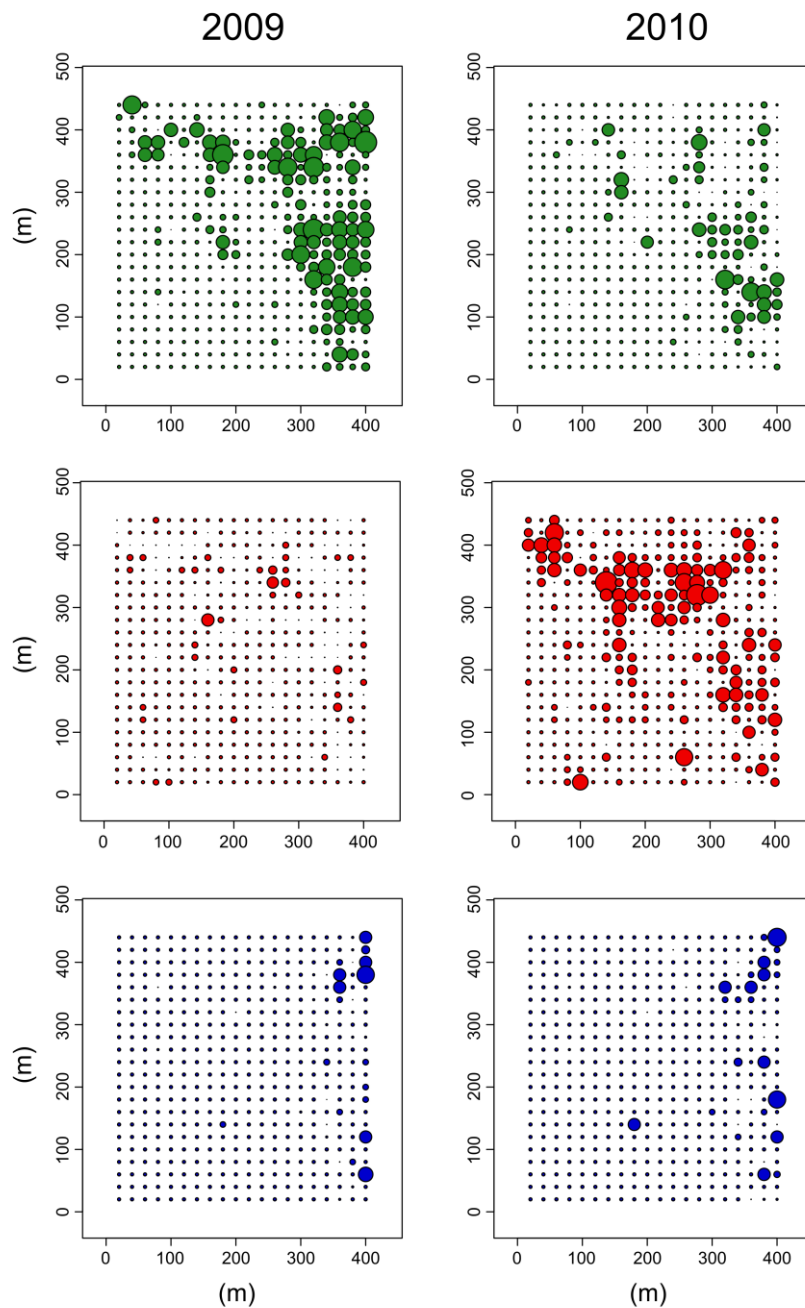
39 while in 2010 we found the opposite trend (Fig.2 and Supplementary Material Appendix
40 1 Fig. A2). Specifically, the number of fruits per square meter per cell for each fruiting
41 tree species (\pm standard deviation) for 2009 and 2010, respectively, was: *C. monogyna*:
42 1.44 ± 0.01 and 12.21 ± 0.05 ; *I. aquifolium*: 14.16 ± 0.06 and 4.81 ± 0.03 ; *T. baccata*:
43 1.27 ± 0.02 and 1.77 ± 0.02 . As a result, and taking into account the spatial distribution
44 whereby *I. aquifolium* and *T. baccata* trees are mainly located in forest patches but *C.*
45 *monogyna* trees are more evenly distributed across the whole study plot (i.e. from larger
46 forest fragments to the deforested matrix), we found a change in the fruiting landscape
47 between years (see also García et al. 2013; Rodríguez-Pérez et al. 2014)

48

49 2. Abundance and foraging patterns of frugivorous thrushes

50 From 2008 to 2011 we recorded the abundance and the foraging behavior of thrushes in
51 our study plot. In order to estimate the abundance, from October to February of each
52 year, we made direct observations from five vantage points located in elevated outcrops
53 (Supplementary Material Appendix 1 Fig. A1.B) in a balanced number of 1-hour
54 observations of all stations. The cumulative yearly observation time was 103, 105, 156
55 and 215 h (for 2008 to 2011 respectively). Due to the denser forest canopy and
56 topographical characteristics of some stations, complementary bird observations were
57 made from 12 forest point-count positions, each one corresponding to the center of a
58 group of four cells (Supplementary Material Appendix 1 Fig. A1.B). These observations
59 were made over 10 min periods, and the cumulative observation time from each point
60 count was 160, 110, 195 and 230 min (for 2008 to 2011, respectively). For each
61 individual thrush, we recorded the species identity and the sampling cell in which it was
62 observed. Our goal was to provide a measure of bird abundance in functional terms, i.e.

63 an estimation of the total activity of the frugivorous thrushes across the season in the
64 plot, rather than estimating their actual population sizes. For more information about
65 this methodology, see García and Martínez (2012), García et al. (2013) and Morales et
66 al. (2013).



67

68 **Figure A2.** Abundance and distribution of fruit crop of the tree species under study (green: *Ilex*
69 *aquifolium*; red: *Crataegus monogyna*; blue: *Taxus baccata*) in the study plot in two different

70 years (2009 and 2010). Dots represent the centroids of each cell and their size is proportional to
71 the number of fruits per cell.

72

73 From 2008 to 2010 we also recorded the foraging behavior and movement
74 patterns of birds in our study plot. From October to February, we gathered data on the
75 activity of thrushes over individual sequences from the five vantage positions described
76 above. Observation time was 90, 79 and 63 h for 2008, 2009 and 2010, respectively.
77 During each census time we recorded (a) the thrush species identity, (b) the flight
78 distance of each movement step (i.e. Euclidean distance between the centroids of the
79 starting point and endpoint cells), (c) the duration and the location of resting time (i.e.
80 the perching tree/landing microhabitat), and (d) the species and number of fleshy fruits
81 consumed while perching in a tree. Individual birds were followed until lost, that is,
82 when they disappeared into the canopy and/or left the study plot.

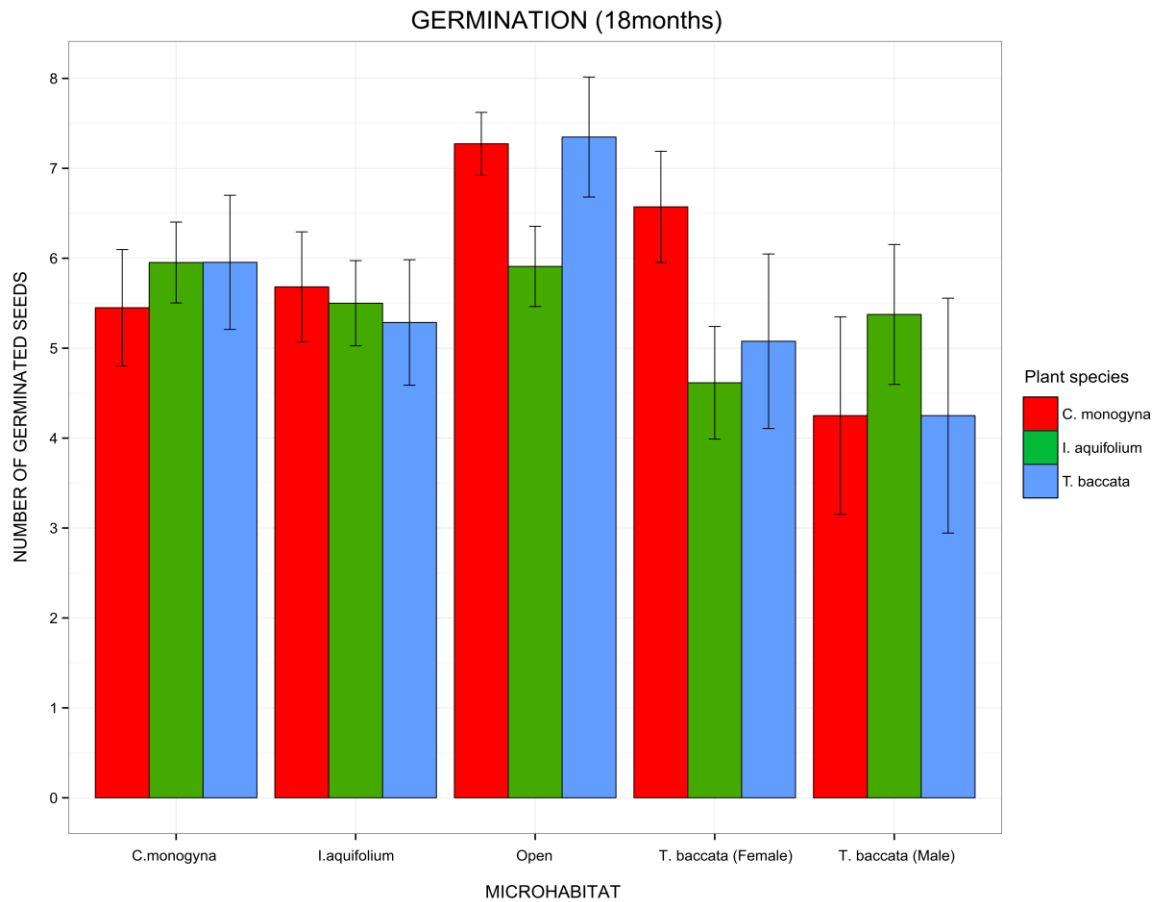
83

84 3. *Seed dispersal*

85 In fall-winter 2009-2010 and 2010-2011 (sampling years 2009 and 2010, hereafter) we
86 quantified seed deposition by thrushes in a subset of 220 cells following a checkered
87 pattern (Supplementary Material Appendix 1 Fig. A1.C). Along the central longitudinal
88 axis of these cells we set up 10 sampling stations separated from each other by 2 m
89 (Supplementary Material Appendix 1 Fig. A1.B). Each sampling station consisted of a
90 50 cm x 50 cm open-ground quadrat where all the seeds dispersed by thrushes were
91 collected and counted (Supplementary Material Appendix 1 Fig. A1.C). Seed surveys
92 took place in late November and early January of each sampling year. Each seed
93 sampling station was assigned to one of the following five possible microhabitats,
94 depending on the type of fine-scale cover: (a) under *C. monogyna*, (b) under *I.*

95 *aquifolium*, (c) under *T. baccata*, (d) under non-fleshy-fruited species (e.g. *Corylus*
96 *avellana*) and (e) in the open (i.e. uncovered by tree canopy, e.g. pastures). Thus, we
97 assessed the number of deposited seeds per tree species per year in each sampling
98 station as being the sum of seeds found in the two consecutive surveys.

99 The germination of the seeds of the studied tree species occurred in the field in
100 the second spring (April to June) following seed dispersal (i.e. after 18 months), with no
101 clear differences between tree species or microhabitat, as suggested by a field
102 germination test conducted in 2004-2005 in an area near the study plot. In this test, sets
103 of 10 seeds recently dispersed by birds and apparently viable (based on checking the
104 fullness of the endocarp by buoyancy) were placed inside 5cm x 5cm glass-fiber bags of
105 1 mm pore diameter. We buried the seed bags in the topsoil surface layer (at a depth of
106 3 cm) in 25 sampling stations per each of the following microhabitats: (a) beneath *C.*
107 *monogyna*, (b) beneath *I. aquifolium*, (c) beneath female *T. baccata*, (d) beneath male *T.*
108 *baccata* and (e) in the open. After 18 months, we retrieved the bags and in the
109 laboratory counted the number of seeds showing signs of germination (i.e. the seed coat
110 was split into two valves or had seedling remains). Slight differences between
111 microhabitats were found only for seeds of *C. monogyna* beneath *C. monogyna* and in
112 the open, and between tree species with regards to the seeds of *I. aquifolium* and *C.*
113 *monogyna* in the open (Fig. A3).



114

115 **Figure A3.** Number of germinated seeds (mean +/- SE) for the different plant species at each of
 116 the five microhabitats after a period of 18 months following seed dispersal by birds.

117

118 *4. Seedling emergence and survival*

119 Seedling emergence and seedling survival surveys took place from April to late August
 120 of 2011 and 2012, so that the emerged seedlings corresponded to the cohorts of seeds
 121 dispersed in our study site in 2009-2010 and 2010-2011, respectively. We set up five
 122 seedling sampling stations distributed in each of the 220 cells, separated by 4 meters
 123 from each other but alongside the seed dispersal sampling stations (Supplementary
 124 Material Appendix 1 Fig. A1.D). During spring-summer we quantified, with a labeled
 125 50 cm x 50 cm quadrat on the ground, the number of seedlings of each of the three
 126 fleshy-fruited tree species of this study which had emerged (*C. monogyna*, *I. aquifolium*

127 and *T. baccata*). Seedlings were individually identified, by assigning to each of them x,y
128 spatial coordinates within the frame of the sampling quadrat, and mapping them on a
129 drawing template. They were aged based on the presence-absence of cotyledons and the
130 stem woodiness (see Peterken and Lloyd, 1967; Thomas and Polwart, 2003). We also
131 determined the microhabitat for each seedling sampling station categorizing them
132 according to the same five microhabitats as for seed sampling stations described above
133 (i.e. under *C. monogyna*, *I. aquifolium*, *T. baccata*, other non-fleshy trees or in open
134 areas). We examined the survival of emerged seedlings monthly during spring and
135 summer, until late August, locating the same individual seedlings across surveys. We
136 considered a seedling to be establishment when it survived until the end of the summer,
137 as previous surveys had revealed that the summer period was the period when most
138 seedling mortality occurred (Martínez 2014).

139

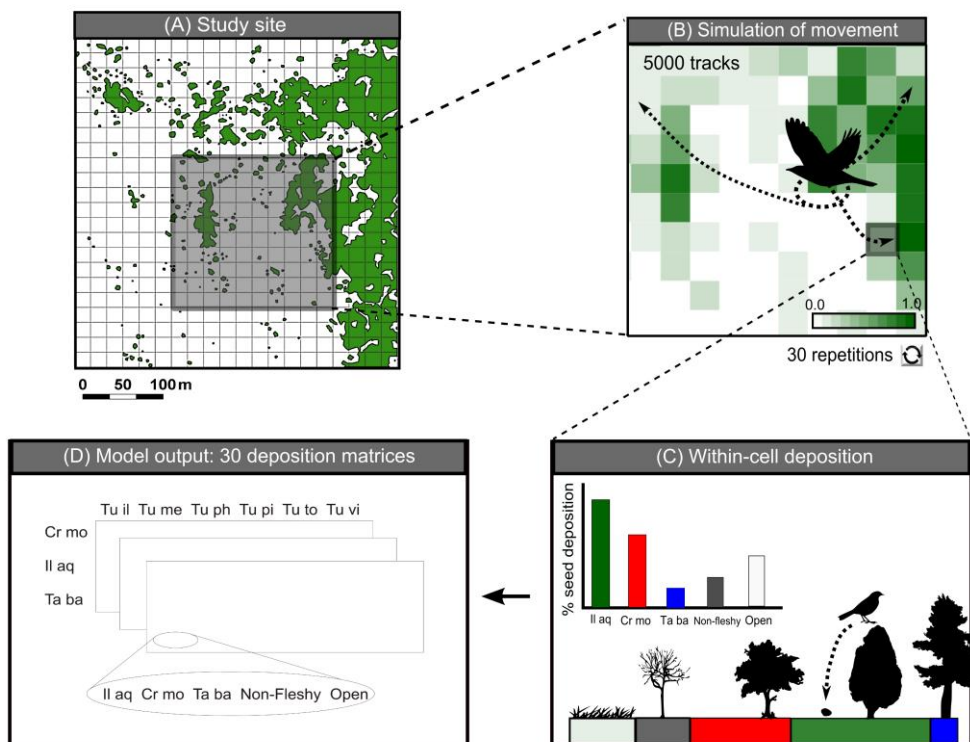
140 REFERENCES

- 141 García, D. and Martínez, D. 2012. Species richness matters for the quality of ecosystem
142 services: a test using seed dispersal by frugivorous birds. - Proc. Biol. Sci. 279: 3106–
143 13.
- 144 García, D. et al. 2013. Functional heterogeneity in a plant-frugivore assemblage
145 enhances seed dispersal resilience to habitat loss. - Ecography 36: 197–208.
- 146 Herrera, J.M. et al. 2011. Regional vs local effects of habitat loss and fragmentation on
147 two plant-animal interactions. - Ecography 34: 606–615.
- 148 Martínez, D. 2014. Seed dispersal and forest recolonization in a fragmented landscape.
149 Looking for the footprint of thrushes (*Turdus* spp.) beyond the forest. PhD thesis,
150 University of Oviedo. Oviedo.
- 151 Morales, J. M. et al. 2013. Frugivore behavioural details matter for seed dispersal: A
152 multi-species model for Cantabrian thrushes and trees. - PLoS One 8: e65216.

- 153 Peterken, G. F. and Lloyd, P. S. 1967. Biological Flora of the British Isles: *Ilex*
154 *aquifolium* L. - J. Ecol. 55: 841–858.
- 155 Rodríguez-Pérez J. et al. 2014. Spatial networks of fleshy-fruited trees drive the flow of
156 avian seed dispersal through landscape. - Funct. Ecol. 28: 990–998.
- 157 Saracco, J.F. et al. 2005. Crop size and fruit neighborhood effects on bird visitation to
158 fruiting *Schefflera morototoni* trees in Puerto Rico. - Biotropica 37:81–87.
- 159 Thomas, P. A. and Polwart, A. (2003). *Taxus baccata* L. - J. Ecol. 91: 489–524.
- 160

161 **Appendix 2 – Model details and parameterization of seed rain for five different**
162 **deposition microhabitats**

163 We adapted the simulation model in Morales et al. (2013) to recreate the relative
164 contribution of each bird species to the total seed rain while moving through a grid-
165 based landscape (see Supplementary Material Appendix 2 Fig. A4). The adapted model
166 includes several rules emulating bird activity and resource tracking. These rules
167 depended on the different spatial behavior of each thrush species and their response to
168 the habitat structure. Thus, they were mainly based on (a) perching time, fruit
169 consumption and gut passage time, (b) movement events and (c) the probability of seed
170 deposition events in different microhabitats. These rules were parameterized for each of
171 the six species of thrushes in order to get a final output: the spatially-explicit and
172 species-specific seed deposition, used to generate a tree-bird seed dispersed interaction
173 matrix.



174

175

176 **Figure A4.** Diagram representing: (A) the distribution of forest cover (green area) in the grid-based study
177 plot divided into cells that replicated the field study plot; (B) a detail showing the proportion of per-cell
178 forest cover represented by the green shading. An example of part of the landscape is plotted with the
179 likely bird movement events and activity (illustrated by arrows). Model simulation is based on 30
180 replicates of 5000 bird tracks; (C) a schematic representation of the probability of seed deposition events
181 (including the probability of perching in the five microhabitats, and the gut passage time) within a given
182 cell; (D) a final mean simulated tree-bird-microhabitat matrix.

183

184 In order to simulate the movement of each bird, our model was fitted to each
185 thrush species based on data obtained from sequences of bird activity made in the study
186 plot from 2008 to 2010 (in which individual birds were tracked by an observer,
187 recording the path followed by the bird and its foraging activity; see Morales et al.
188 2013). The model aims to predict the seed dispersal patterns that emerge from the
189 interplay between thrush abundance and their response to the spatial heterogeneity of
190 habitat cover and fruit availability. Given the strong inter-annual differences in fruit
191 abundance and distribution typical in this study system (García et al. 2013; see also
192 Supplementary Material Appendix 1, Fig. A2), we used the data of both 2009 and 2010
193 to fit those model functions related to the number of fruits. The remaining functions,
194 which do not depend on habitat heterogeneity (e.g. distance to the nearest plot border,
195 see below), were fitted also taking into account data from 2008 in order to achieve a
196 bigger sample size.

197 The calculations described below (i.e. eq. A1, A2, A3 and A4) were used, first,
198 to estimate the values of the parameters needed to build the rules of the mechanistic
199 model. Our mechanistic rules were a combination of mathematical functions describing
200 the performance of each bird species depending on each bird movement, and activity
201 during fruit supply. These mathematical functions had different parameters, i.e. constant
202 values that determined the shape of the function, which varied between thrush species.

203 The parameters were estimated by fitting different probability density distributions to
 204 field data. In other words, the probability that a given event would, (or would not),
 205 occur during the activity of each bird (see Supplementary Material Appendix 2 Fig. A5
 206 and Fig. A6). To obtain maximum-likelihood estimates for each parameter, we
 207 minimized the negative log-likelihood functions using the Nelder-Mead algorithm
 208 (Nelder and Mead 1965) with several overdispersed starting points using the *bbmle*
 209 library (Bolker and R Development Core Team 2014). The model was implemented in
 210 R statistical language (R Development Core Team 2014). Below we describe the
 211 general simulation procedure and how we parameterized the mechanistic rules.

212 *a) Perching time and fruit consumption*

213 Every time a simulated bird arrived to a landscape cell, it spent an amount of time there
 214 drawn from a Gamma distribution fitted to the observed perching time for each species.
 215 The time a bird was in a given cell was independent of fruit consumption in it, as there
 216 is no existing evidence relating to this fact (Morales et al. 2013 and Supplementary
 217 Material Appendix 2 Table A1). The decisions of the simulated birds (i.e. to stay or to
 218 leave to go to a new landscape cell) were made once perching time expired.

219 **Table A1.** Pearson's product-moment correlations between perching time and fruit
 220 consumption for each species.

	r	t and df	p - value	CI
<i>Turdus iliacus</i>	0.084	t = 0.7441, df = 78	0.459	-0.138 0.459
<i>Turdus merula</i>	-0.110	t = -1.0576, df = 91	0.293	-0.307 0.096
<i>Turdus philomelos</i>	0.487	t = 2.494, df = 20	0.021	0.082 0.754
<i>Turdus pilaris</i>	-0.262	t = -0.470, df = 3	0.671	-0.929 0.807
<i>Turdus torquatus</i>	-0.426	t = -0.943 , df = 4	0.340	-0.920 0.589

Turdus viscivorus -0.004 t = -0.040, df =86 0.968 -0.214 0.205

221

222 Frugivory events depended on both the fruit availability in a given cell and
223 observed fruit consumption rates (García et al. 2013). Simulated birds potentially
224 consumed fruits based on a zero-inflated Poisson distribution fitted to the observed
225 number of fruits consumed by each bird species, and they had no built-in fruit species
226 preferences. Plant species identity depended on fruit species abundance in the landscape
227 cell (Morales et al 2013). If the number of potentially fruits consumed was higher than
228 the number of fruits available in the landscape cell, the simulated birds consumed the
229 minimum between the above-mentioned values.

230 *b) Movement events*

231 When perching time expired, the movements of simulated birds depended on three main
232 decisions, namely whether to: (i) stay in the same landscape cell, (ii) move to a new
233 cell, or (iii) leave the study plot. First, the model computed the probability of leaving
234 the study plot (v) based on the distance to the nearest plot border (B):

$$235 \quad \text{logit}(v) = a_0 + b_0B \quad (\mathbf{A1})$$

236 where a_0 and b_0 are parameters fitted to each bird species based on observed data. Given
237 that the previous (i) rule is independent of habitat heterogeneity (e.g. distance to the
238 nearest plot border, see below), we included the observational data for 2008, with the
239 aim of assuring a larger sample size when fitting the model functions of each bird
240 species.

241 Second, if simulated birds decided to stay in the plot, their decisions were
242 affected by; (i) distance between the current and the destination cell, (ii) the proportion

243 of forest cover, and (iii) the number of fruits at the destination cell. Thus, the model
 244 computed a discrete probability distribution based on hyperbolic tangent functions [*tanh*
 245 (*x*)] as follows:

$$\begin{aligned}
 d_i &= 1 - \tanh\left(\left(\delta_{ij}/a_d\right)^{b_d}\right) \\
 c_i &= \tanh\left(\left(\text{cover}_i/a_c\right)^{b_c}\right) \\
 f_i &= \tanh\left(\left(\log(\text{fruit}_i + 1)/a_f\right)^{b_f}\right) \\
 \mathbf{k} &= \frac{[\mathbf{d} \otimes \mathbf{c} \otimes \mathbf{f}]}{\sum[\mathbf{d} \otimes \mathbf{c} \otimes \mathbf{f}]}
 \end{aligned}
 \tag{A2}$$

246 where the scale (i.e. a_d , a_c and a_f) and shape parameters (i.e. b_d , b_c and b_f) control the
 247 shape of the probability between factors. These scale and shape parameters were
 248 estimated for each bird species based on observed bird trajectories, forest cover and fruit
 249 abundances (Morales et al. 2013). The vectors \mathbf{d} , \mathbf{c} and \mathbf{f} carry the probability of
 250 choosing the i -th landscape cell depending on the distance to current location (d), forest
 251 cover (c) and fruit abundance (f), and they are multiplied in order to achieve a discrete
 252 probability vector, \mathbf{k} , of choosing landscape cells. Once the simulated birds decided
 253 where to go, they flew at a constant speed of 6 m s^{-1} , following a straight line and the
 254 Euclidean distance from the perch of origin to the destination perch. A maximum
 255 number of six movements per track were permitted, as $> 95\%$ of sequences recorded in
 256 the field were at or below that threshold.

257 *c) Seed deposition events in microhabitats*

258 Furthermore, we implemented the rules to predict seed deposition events into specific
 259 microhabitats, as a mechanism combining (i) perching probability in the five
 260 microhabitats and (ii) gut-passage time. The microhabitats considered in the current
 261 version were; (a) under *C. monogyna*, (b) under *I. aquifolium*, (c) under *T. baccata*, (d)
 262 under non-fleshy-fruited tree species and (e) in open microhabitat (e.g. pastures)

263 (Supplementary Material Appendix 2 Fig. A6). For each simulated track and cell, and
264 considering those microhabitats including fleshy-fruited tree species, the perch
265 probability depended on; (1) the foraging activity (based on fruit consumption and
266 movement across the landscape), (2) the number of fleshy fruits in a given cell, and (3)
267 the number of individuals of each tree species in a given cell (Supplementary Material
268 Appendix 2 Fig. A6). The perching probability (k) depending on the number of fruits
269 (B) and trees (C) is thus as follows:

$$270 \quad \text{logit}(k) = a_o + b_o B + c_o C \quad (\mathbf{A3})$$

271 where a_o , b_o and c_o are parameters fitted to each bird species based on observed data. In
272 the case of depositions beneath non-fleshy-fruited trees or in open microhabitat, the
273 perching probability (k) in relation to the number of non-fleshy fruited trees or the
274 proportion of forest cover (B) is as follows:

$$275 \quad \text{logit}(k) = a_o + b_o B \quad (\mathbf{A4})$$

276 where a_o and b_o are parameters fitted to each bird species. For each microhabitat and
277 bird species, we thus obtained estimates from the best model and generated perching
278 probability events based on logistic distributions (Supplementary Material Appendix 2
279 Fig. A6).

280 Secondly and based on previous studies in the same area and study system
281 (García et al. 2007), we considered that seeds of a given tree species had a higher
282 probability of arrival beneath the microhabitat representing a tree of that same species
283 (i.e. deposition under conspecifics). We therefore considered the probability of perching
284 in conspecifics (i.e. the same fleshy-fruited species previously consumed) as 0.4, 0.8
285 and 0.5 for *C. monogyna*, *I. aquifolium* *T. baccata*, respectively. In essence, this rule
286 mimics a phenomenological matching between the fruiting time of each tree species and

287 its higher perching probability in conspecifics, which may be a consequence of the more
 288 limited crop of the other fleshy-fruited species at that time.

289 For every frugivore event, ingested seeds have a certain gut-passage time (GPT)
 290 inside the bird. GPT distributions were fitted to empirical data based on experimental
 291 retention times of 18 hand-raised and captive wild specimens of *Turdus merula* (Sobral,
 292 Larrinaga and Santamaría, *unpublished data*). GPTs were drawn from a Gamma
 293 distribution with a common shape parameter (i.e. 1.59), but a bird species-specific scale
 294 parameter (i.e. 0.029 to 0.074; Supplementary Material Appendix 2 Table A2) based on
 295 the relationship between the body size and GPT of each *Turdus* species, using eight
 296 species from *Turdidae* and *Sylviidae* (Herrera 1984; see Morales et al. 2013).

297 **Table A2.** Coefficients of GPT for different species of thrushes based on body size and
 298 with reference to *Turdus merula* GPT.

Species	Body size (g)*	mean GPT estimate	Rate for Gamma distribution†
<i>T. iliacus</i>	65	21.45	0.0740
<i>T. merula</i>	100	39.34	0.0400
<i>T. philomelos</i>	75	26.57	0.0598
<i>T. pilaris</i>	110	44.45	0.0357
<i>T. torquatus</i>	120	49.56	0.0320
<i>T. viscivorus</i>	130	54.67	0.0290

299 * From Collar (2005)

300 † Assuming the shape parameter is 1.59, the same as in the Gamma distribution fitted to the data from
 301 *Turdus merula* in Morales *et al.* 2013.

302

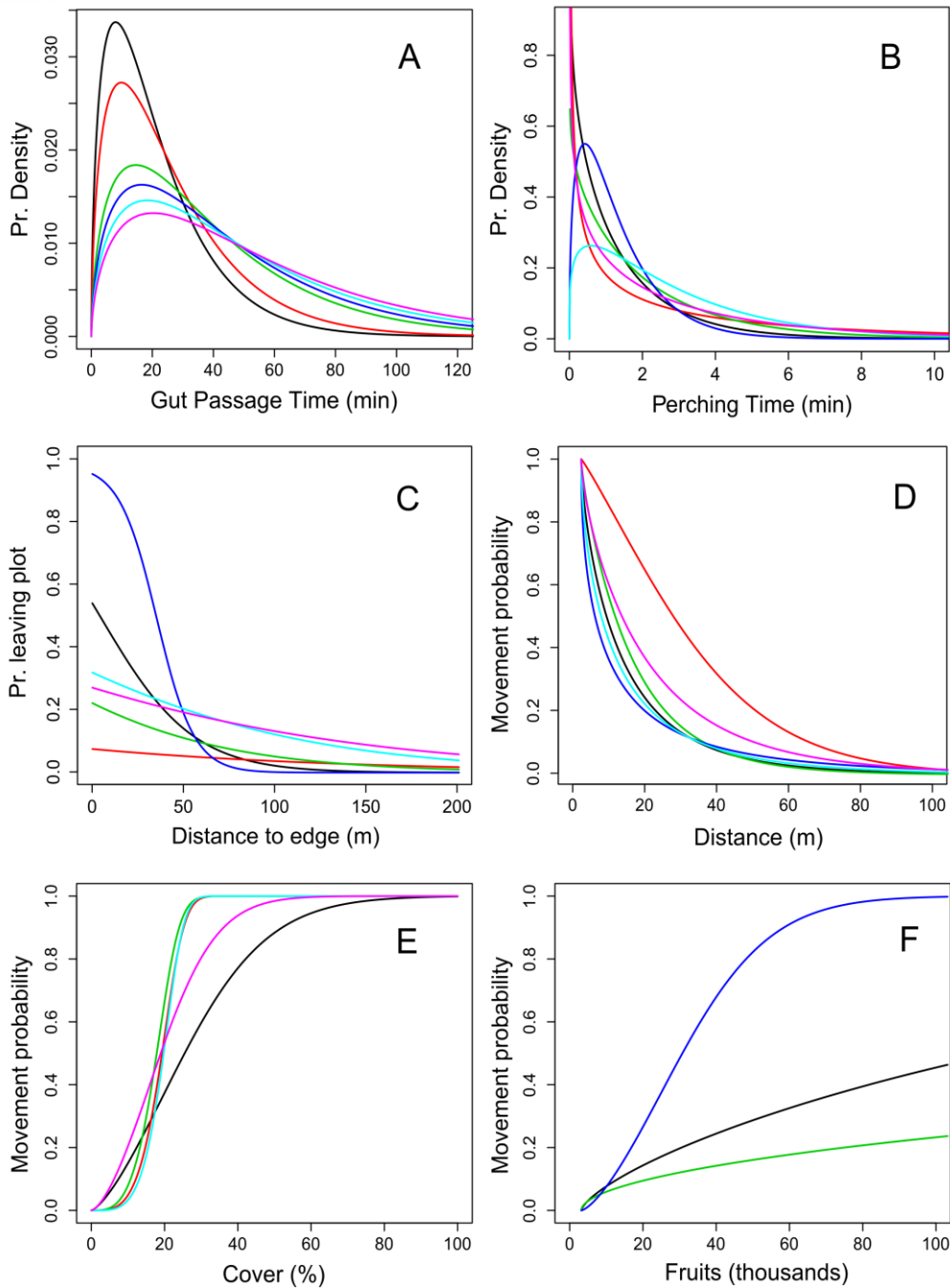
303 Finally, seed deposition events in the five microhabitats occurred once frugivory
 304 and perching had occurred, and once gut-passage time had expired. Each simulated bird
 305 deposited all the seeds consumed in a single deposition event. The number of seeds per
 306 deposition was always considered to be one, except for *I. aquifolium*, where the number

307 of seeds deposited was corrected to account for the probability of having between 1 and
308 4 seeds per fruit, based on Obeso (1998).

309 *d) General considerations and model output*

310 We obtained each model output (i.e. seed deposition data) as a spatially-explicit (cell-
311 and microhabitat-based) prediction of seed deposition for each tree species and by each
312 bird species, that is, a multi-specific seed rain across the modeled landscape. Each
313 model output was the result of a simulation accounting for 5000 bird tracks, and the
314 simulations were replicated 30 times (i.e. 30 independent model outputs), for each of
315 the two different year scenarios (2009 and 2010). These year scenarios accounted for
316 the field-based values of fruit availability and bird abundance of the different species in
317 the respective years. We finally selected the seed deposition output corresponding to a
318 subset of 220 cells of the modeling landscape, in equivalent positions to those
319 containing seed deposition and seedling establishment sampling stations in the field
320 (Supplementary material Appendix 1, Fig. A1.C).

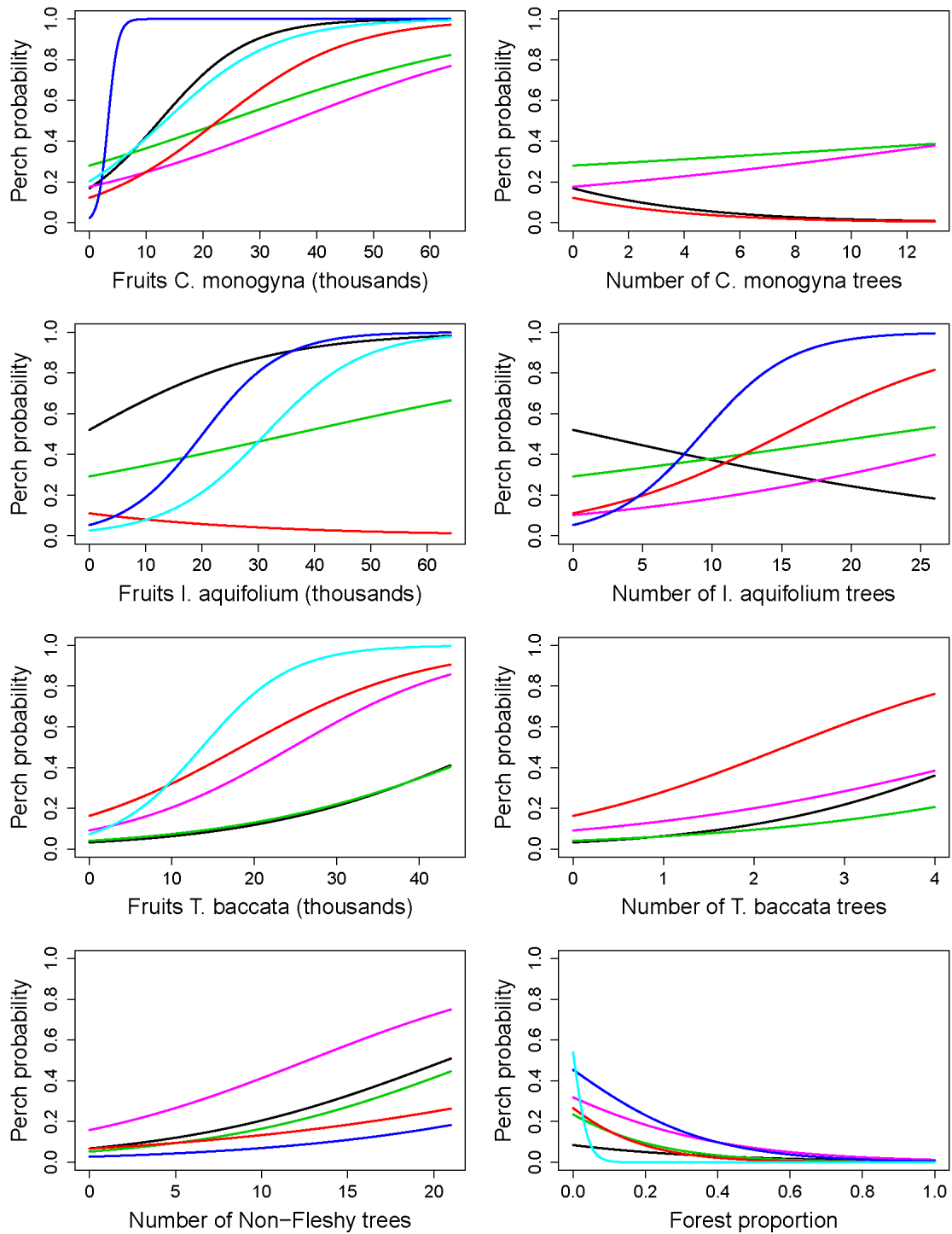
321 The data of each seed deposition output, accounting for tree-bird and tree-
322 microhabitat specific information, were pooled across microhabitats. In this way we
323 obtained a seed deposition matrix which accounted for the number of seeds of each of
324 the different tree species which were dispersed by each bird species. For each year
325 scenario, we thus obtained 30 matrices of simulated seed deposition (Fig. 1D).



326

327 **Figure A5.** Model functions fitted to different species of thrushes for perching time, movement
 328 probabilities and gut-passage time. Gut-passage time (A) is Gamma distributed with scale parameter
 329 related to bird size. Perching time (B) is Gamma distributed and fitted to data from direct observations.
 330 The probability of leaving the study plot (C) decreased with distance to the plot edge. Movement to
 331 another landscape cell (D) decreased with increased distance to that cell. Movement probability increased
 332 with forest cover and with fruits (E and F). The species of thrushes are: *Turdus iliacus* (black), *T.*
 333 *philomelos* (red), *T. merula* (green), *T. pirus* (blue), *T. torquatus* (cyan) and *T. viscivorus* (magenta). (A)
 334 and (C) were fitted with observational data collected during 2007, 2008, 2009, 2010, as in Morales et al
 335 (2013); (B) during 2008, 2009, 2010; and (D), (E), and (F) with observational data collected during 2009,
 336 2010 because they corresponded to functions depending on landscape characteristics and, thus, could vary
 337 between years.

338



339

340 **Figure A6.** Mechanistic functions describing perching probability beneath microhabitats for each *Turdus*
 341 species. For each microhabitat, we calculated perching probability as a function of fruits and number of
 342 trees of *C. monogyna* (first row), *I. aquifolium* (second row), and *T. baccata* (third row). For non-fleshy-
 343 fruited trees (fourth row, left) deposition probabilities only depended on the number of trees, whereas the
 344 probability of deposition in the open (fourth row, right) was calculated as a function of the proportion of
 345 forest cover. The *Turdus* species are: *T. iliacus* (black), *T. philomelos* (red), *T. merula* (green), *T. piralis*
 346 (blue), *T. torquatus* (cyan) and *T. viscivorus* (magenta).

347

348 **REFERENCES**

- 349 Bolker B. and R Development Core Team 2014. *bbmle*: Tools for general maximum
350 likelihood estimation. -R package version 1.0.17. [http://CRAN.R-](http://CRAN.R-project.org/package=bbmle)
351 [project.org/package=bbmle](http://CRAN.R-project.org/package=bbmle)
- 352 Collar, N. J. 2005. Family Turdidae (Thrushes). Pp. 514-807 in del Hoyo, J., Elliot, A.
353 & Christie, D. A. Handbook of the Birds of the World. Vol. 10. Cuckoo-shrikes to
354 Thrushes. Lynx Edicions, Barcelona.
- 355 García, D. et al. 2007. Seed transfer among bird-dispersed trees and its consequences
356 for post-dispersal seed fate. - Basic Appl. Ecol. 8: 533–543
- 357 García, D. et al. 2013. Functional heterogeneity in a plant-frugivore assemblage
358 enhances seed dispersal resilience to habitat loss. - Ecography 36: 197–208
- 359 Herrera, C.M. 1984. Adaptation to frugivory of Mediterranean avian seed dispersers. -
360 Ecology 65: 609–617
- 361 Morales, J. M. et al. 2013. Frugivore behavioural details matter for seed dispersal: A
362 multi-species model for Cantabrian thrushes and trees. - PLoS One 8: e65216.
- 363 Nelder, J.A. and Mead, R. 1965. A simplex method for function minimization. -
364 *Computer Journal*. 7: 303-313
- 365 Obeso, J.R. 1998. Patterns of variation in *Ilex aquifolium* fruit traits related to fruit
366 consumption by birds and seed predation by rodents. - EcoScience 5 (4): 463-469
- 367 R Development Core Team 2013. R: a Language and Environment for Statistical
368 Computing. R Foundation for Statistical Computing, Vienna.
- 369

370 **Appendix S3 – Matrices**

371 **Table A3. Tree-microhabitat observed seed deposition matrices.** Relative abundance of seeds (in %) of different tree species (rows) deposited
 372 by frugivorous birds in different microhabitats (columns) for 2009 (a) and 2010 (b). The total number of observed seeds per fleshy-fruited tree
 373 species under study is specified in the last column.

374

(a) 2009	Under <i>C. monogyna</i>	Under <i>I. aquifolium</i>	Under <i>T. baccata</i>	Under non-fleshy-fruited tree	Open	No. seeds
<i>Crataegus. monogyna</i>	30.46	40.61	5.31	14.99	8.62	847
<i>Ilex aquifolium</i>	9.58	69.56	2.28	12.69	5.88	32131
<i>Taxus baccata</i>	18.49	27.92	35.89	11.62	6.07	1368

375

376

(b) 2010	Under <i>C. monogyna</i>	Under <i>I. aquifolium</i>	Under <i>T. baccata</i>	Under non-fleshy-fruited tree	Open	No. seeds
<i>Crataegus. monogyna</i>	29.75	47.98	4.22	6.53	11.52	3126
<i>Ilex aquifolium</i>	15.46	70.23	6.59	5.09	2.63	9477
<i>Taxus baccata</i>	5.03	24.82	54.17	7.14	8.84	2228

377

378 **Table A4. Tree-microhabitat first transition probability.** *Seedling emergence rates* for the different tree species (rows) in different
 379 microhabitats (columns), corresponding to two seed cohorts, 2009 (a) and 2010 (b). *Seedling emergence rates* were calculated as the proportion
 380 of dispersed seeds from which a seedling emerged after an 18 months post-dispersal period.

381

(a) 2009	Under <i>C. monogyna</i>	Under <i>I. aquifolium</i>	Under <i>T. baccata</i>	Under non-fleshy-fruited tree	Open
<i>Crataegus. monogyna</i>	1.000	0.493	0.364	0.370	1.000
<i>Ilex aquifolium</i>	0.117	0.049	0.109	0.100	0.476
<i>Taxus baccata</i>	0.077	0.017	0.017	0.238	0.000

382

383

(b) 2010	Under <i>C. monogyna</i>	Under <i>I. aquifolium</i>	Under <i>T. baccata</i>	Under non-fleshy-fruited tree	Open
<i>Crataegus. monogyna</i>	0.789	0.324	0.364	0.622	1.000
<i>Ilex aquifolium</i>	0.192	0.168	0.093	0.809	1.000
<i>Taxus baccata</i>	0.042	0.082	0.008	0.050	0.062

384

385 **Table A5. Tree-microhabitat second transition probability.** *Seedling survival rates* for different tree species (rows) in different microhabitats
 386 (columns), corresponding to two seed cohorts, 2009 (a) and 2010 (b). *Seedling survival rates* were calculated as the proportion of emerged
 387 seedlings which survived to the end of the summer season.

388

(a) 2009	Under <i>C. monogyna</i>	Under <i>I. aquifolium</i>	Under <i>T. baccata</i>	Under non-fleshy-fruited tree	Open
<i>Crataegus. monogyna</i>	0.386	0.413	0.250	0.500	0.458
<i>Ilex aquifolium</i>	0.550	0.352	0.461	0.516	0.193
<i>Taxus baccata</i>	1.000	0.500	0.500	0.500	0.000

389

(b) 2010	Under <i>C. monogyna</i>	Under <i>I. aquifolium</i>	Under <i>T. baccata</i>	Under non-fleshy-fruited tree	Open
<i>Crataegus. monogyna</i>	0.224	0.247	0.125	0.357	0.295
<i>Ilex aquifolium</i>	0.516	0.390	0.500	0.436	0.203
<i>Taxus baccata</i>	1.000	0.143	0.333	0.273	0.000

390

391

392 **Table A6. Tree-microhabitat predicted seed deposition matrices.** Relative abundance of simulated seeds (in %) of the different tree species
 393 (rows) deposited by frugivorous birds in different microhabitats (columns) for 2009 (a) and 2010 (b).

394

(a) 2009	Under <i>C. monogyna</i>	Under <i>I. aquifolium</i>	Under <i>T. baccata</i>	Under non-fleshy-fruited tree	Open	No. seeds
<i>Crataegus. monogyna</i>	34.76	31.25	11.72	10.94	11.33	256
<i>Ilex aquifolium</i>	2.70	90.73	3.01	2.26	1.30	3227
<i>Taxus baccata</i>	7.32	31.71	43.90	12.19	4.88	41

395

(b) 2010	Under <i>C. monogyna</i>	Under <i>I. aquifolium</i>	Under <i>T. baccata</i>	Under non-fleshy-fruited tree	Open	No. seeds
<i>Crataegus. monogyna</i>	43.11	22.17	17.20	8.57	8.95	1610
<i>Ilex aquifolium</i>	4.03	87.15	4.50	3.09	1.23	1712
<i>Taxus baccata</i>	9.65	18.42	59.65	8.77	3.51	114

396

397

398 **Table A7. Tree-microhabitat predicted seedling recruitment matrices.** Relative abundance of simulated seedlings (in %) of the different
 399 tree species (rows) recruited by frugivorous birds in different microhabitats (columns) for 2009 (a) and 2010 (b). The total number of predicted
 400 seedling recruited per tree species is specified in the last column.

401

(a) 2009	Under <i>C. monogyna</i>	Under <i>I. aquifolium</i>	Under <i>T. baccata</i>	Under non-fleshy-fruited tree	Open	No. seedlings
<i>Crataegus. monogyna</i>	47.89	22.54	4.22	7.04	18.31	71
<i>Ilex aquifolium</i>	8.69	72.46	7.25	5.80	5.80	69
<i>Taxus baccata</i>	50.00	0.00	0.00	50.00	0.00	2

402

(a) 2010	Under <i>C. monogyna</i>	Under <i>I. aquifolium</i>	Under <i>T. baccata</i>	Under non-fleshy-fruited tree	Open	No. seedlings
<i>Crataegus. monogyna</i>	52.13	11.97	5.13	12.82	17.95	234
<i>Ilex aquifolium</i>	5.35	74.81	2.29	14.50	3.05	131
<i>Taxus baccata</i>	100.00	00.00	0.00	0.00	0.00	1

403

404 **Table A8. Bird-microhabitat predicted seed deposition matrices.** Relative abundance of seeds (in %) deposited by each of the frugivorous
 405 bird species (rows) in the different microhabitats (columns) for 2009 (a) and 2010 (b). The total number of predicted seeds deposited by each
 406 bird species is specified in the last column.

407

(a) 2009	Under <i>C. monogyna</i>	Under <i>I. aquifolium</i>	Under <i>T. baccata</i>	Under non-fleshy-fruited tree	Open	No. seeds
<i>T. iliacus</i>	2.74	93.85	1.27	1.81	0.33	1495
<i>T. merula</i>	8.56	86.24	2.01	1.51	1.68	596
<i>T. viscivorus</i>	10.45	70.65	3.98	9.95	4.97	201
<i>T. philomelos</i>	5.34	78.29	8.74	3.81	3.82	1179
<i>T. pilaris</i>	0.00	94.12	0.00	0.00	5.88	17
<i>T. torquatus</i>	8.57	65.71	8.57	14.29	2.86	35

408

409 **Table A8 cont. Bird-microhabitat predicted seed deposition matrices.** Relative abundance of seeds (in %) deposited by each of the
 410 frugivorous bird species (rows) in the different microhabitats (columns) for 2009 (a) and 2010 (b). The total number of predicted seeds
 411 deposited by each bird species is specified in the last column.

412

(b) 2010	Under <i>C. monogyna</i>	Under <i>I. aquifolium</i>	Under <i>T. baccata</i>	Under non-fleshy-fruited tree	Open	No. seeds
<i>T. iliacus</i>	25.54	65.76	3.26	4.35	1.09	184
<i>T. merula</i>	31.60	58.84	2.49	3.95	3.12	481
<i>T. viscivorus</i>	29.10	44.44	6.88	12.17	7.41	189
<i>T. philomelos</i>	19.76	53.87	15.29	5.74	5.34	2545
<i>T. pilaris</i>	50.00	41.67	0.00	0.00	8.33	12
<i>T. torquatus</i>	45.46	27.27	9.09	18.18	0.00	22

413

414

415

416 **Table A9. Bird-microhabitat predicted seedling recruitment matrices.** Relative abundance of seedlings (in %) recruited by each of the
 417 frugivorous bird species (rows) in the different microhabitats (columns) for 2009 (a) and 2010 (b). The total number of predicted seedlings
 418 recruited by each bird species is specified in the last column.

419

(a) 2009	Under <i>C. monogyna</i>	Under <i>I. aquifolium</i>	Under <i>T. baccata</i>	Under non-fleshy-fruited tree	Open	No. seedlings
<i>T. iliacus</i>	21.28	68.09	2.13	4.25	4.25	47
<i>T. merula</i>	44.45	40.74	3.70	3.70	7.41	27
<i>T. viscivorus</i>	40.00	20.00	0.00	20.00	20.00	10
<i>T. philomelos</i>	25.00	35.72	10.71	8.93	19.64	56
<i>T. pilaris</i>	33.33	33.33	0.00	0.00	33.33	3
<i>T. torquatus</i>	20.00	20.00	20.00	20.00	20.00	5

420

421

422 **Table A9 cont. Bird-microhabitat predicted seedling recruitment matrices.** Relative abundance of seedlings (in %) recruited by each of the
 423 frugivorous bird species (rows) in the different microhabitats (columns) for 2009 (a) and 2010 (b). The total number of predicted seedlings
 424 recruited by each bird species is specified in the last column.

425

(b) 2010	Under <i>C. monogyna</i>	Under <i>I. aquifolium</i>	Under <i>T. baccata</i>	Under non-fleshy-fruited tree	Open	No. seedlings
<i>T. iliacus</i>	44.44	44.44	0.00	11.11	0.00	18
<i>T. merula</i>	49.06	35.85	0.00	7.55	7.55	53
<i>T. viscivorus</i>	37.50	20.83	0.00	25.00	16.67	24
<i>T. philomelos</i>	31.83	34.83	5.62	13.48	14.23	267
<i>T. pilaris</i>	100.00	0.00	0.00	0.00	0.00	1
<i>T. torquatus</i>	66.66	0.00	0.00	33.33	0.00	3

426